favorable antiviral efficacy for HIV-1-infected individuals should merit further study.

ACKNOWLEDGMENTS

This work was supported in part by a grant-in-aid for scientific research (priority areas) from the Ministry of Education, Culture, Sports, Science, and Technology of Japan (Monbu-Kagakusho); a grant to the Cooperative Research Project on Clinical and Epidemiological Studies of Emerging and Reemerging Infectious Diseases (Renkei Jigyo; no. 78, Kumamoto University) of Monbu-Kagakusho (H.M.); a grant for the promotion of AIDS research from the Ministry of Health, Welfare, and Labor of Japan (Kosei-Rohdosho; H15-AIDS-001); a grant-in-aid from the Institute of Health Sciences, Kumamoto Health Science University (M.A.); and in part by the intramural research program of the Center for Cancer Research, National Cancer Institute, National Institutes of Health.

REFERENCES

1. **Amano, M., Y. Koh, D. Das, J. Li, S. Leschenko, Y. F. Wang, P. I. Boross, I. T. Weber, A. K. Ghosh, and H. Mitsuya.** 2007. A novel bis-tetrahydrofuranylurethane-containing nonpeptidic protease inhibitor (PI), GRL-98065, is potent against multiple-PI-resistant human immunodeficiency virus in vitro. Antimicrob. Agents Chemother. **51:**2143–2155.
2. **Bally, F., R. Martinez, S. Peters, P. Sudre, and A. Telenti.** 2000. Polymorphism of HIV type 1 gag p7/p1 and p1/p6 cleavage sites: clinical significance and implications for resistance to protease inhibitors. AIDS Res. Hum. Retrovir. **16:**1209–1213.
3. **Bhaskaran, K., O. Hamouda, M. Sannes, F. Boufassa, A. M. Johnson, P. C. Lambert, and K. Porter.** 2008. Changes in the risk of death after HIV seroconversion compared with mortality in the general population. JAMA **300:**51–59.
4. **Braaten, D., and J. Luban.** 2001. Cyclophilin A regulates HIV-1 infectivity, as demonstrated by gene targeting in human T cells. EMBO J. **20:**1300–1309.
5. **Carrillo, A., K. D. Stewart, H. L. Sham, D. W. Norbeck, W. E. Kohlbrenner, J. M. Leonard, D. J. Kempf, and A. Molla.** 1998. In vitro selection and characterization of human immunodeficiency virus type 1 variants with increased resistance to ABT-378, a novel protease inhibitor. J. Virol. **72:**7532–7541.
6. **Clavel, F., and A. J. Hance.** 2004. HIV drug resistance. N. Engl. J. Med. **350:**1023–1035.
7. **Colonno, R., R. Rose, C. McLaren, A. Thiry, N. Parkin, and J. Friborg.** 2004. Identification of I50L as the signature atazanavir (ATV)-resistance mutation in treatment-naive HIV-1-infected patients receiving ATV-containing regimens. J. Infect. Dis. **189:**1802–1810.
8. **Doyon, L., G. Croteau, D. Thibeault, F. Poulin, L. Pilote, and D. Lamarre.** 1996. Second locus involved in human immunodeficiency virus type 1 resistance to protease inhibitors. J. Virol. **70:**3763–3769.
9. **Eron, J. J., S. L. Benoit, J. Jemsek, R. D. MacArthur, J. Santana, J. B. Quinn, D. R. Kuritzkes, M. A. Fallon, and M. Rubin for the North American HIV Working Party.** 1995. Treatment with lamivudine, zidovudine, or both in HIV-positive patients with 200 to 500 CD4+ cells per cubic millimeter. N. Engl. J. Med. **333:**1662–1669.
10. **Eron, J. J., R. Haubrich, W. Lang, G. Pagano, J. Millard, J. Wolfram, W. Snowden, L. Pedneault, and M. Tisdale.** 2001. A phase II trial of dual protease inhibitor therapy: amprenavir in combination with indinavir, nelfinavir, or saquinavir. J. Acquir. Immune Defic. Syndr. **26:**458–461.
11. **Gallego, O., C. de Mendoza, A. Corral, and V. Soriano.** 2003. Changes in the human immunodeficiency virus p7-p1-p6 gag gene in drug-naive and pretreated patients. J. Clin. Microbiol. **41:**1245–1247.
12. **Gamble, T. R., F. F. Vajdos, S. Yoo, D. K. Worthylake, M. Houseweart, W. I. Sundquist, and C. P. Hill.** 1996. Crystal structure of human cyclophilin A bound to the amino-terminal domain of HIV-1 capsid. Cell **87:**1285–1294.
13. **Ganser-Pornillos, B. K., A. Cheng, and M. Yeager.** 2007. Structure of full-length HIV-1 CA: a model for the mature capsid lattice. Cell **131:**70–79.
14. **Gatanaga, H., D. Das, Y. Suzuki, D. D. Yeh, K. A. Hussain, A. K. Ghosh, and H. Mitsuya.** 2006. Altered HIV-1 Gag protein interactions with cyclophilin A (CypA) on the acquisition of H219Q and H219P substitutions in the CypA binding loop. J. Biol. Chem. **281:**1241–1250.
15. **Gatanaga, H., Y. Suzuki, H. Tsang, K. Yoshimura, M. F. Kavlick, K. Nagashima, R. J. Gorelick, S. Mardy, C. Tang, M. F. Summers, and H. Mitsuya.** 2002. Amino acid substitutions in Gag protein at non-cleavage sites are indispensable for the development of a high multitude of HIV-1 resistance against protease inhibitors. J. Biol. Chem. **277:**5952–5961.
16. **Grabar, S., C. Pradier, E. Le Corfec, R. Lancar, C. Allavena, M. Bentata, P. Berlureau, C. Dupont, P. Fabbro-Peray, I. Poizot-Martin, and D. Costagliola.** 2000. Factors associated with clinical and virological failure in patients receiving a triple therapy including a protease inhibitor. AIDS **14:**141–149.
17. **Gross, I., H. Hohenberg, C. Huckhagel, and H. G. Krausslich.** 1998. N-terminal extension of human immunodeficiency virus capsid protein converts the in vitro assembly phenotype from tubular to spherical particles. J. Virol. **72:**4798–4810.
18. **Hatziioannou, T., D. Perez-Caballero, S. Cowan, and P. D. Bieniasz.** 2005. Cyclophilin interactions with incoming human immunodeficiency virus type 1 capsids with opposing effects on infectivity in human cells. J. Virol. **79:**176–183.
19. **Koh, Y., S. Matsumi, D. Das, M. Amano, D. A. Davis, J. Li, S. Leschenko, A. Baldridge, T. Shioda, R. Yarchoan, A. K. Ghosh, and H. Mitsuya.** 2007. Potent inhibition of HIV-1 replication by novel non-peptidyl small molecule inhibitors of protease dimerization. J. Biol. Chem. **282:**28709–28720.
20. **Koh, Y., H. Nakata, K. Maeda, H. Ogata, G. Bilcer, T. Devasamudram, J. F. Kincaid, P. Boross, Y. F. Wang, Y. Tie, P. Volarath, L. Gaddis, R. W. Harrison, I. T. Weber, A. K. Ghosh, and H. Mitsuya.** 2003. Novel bis-tetrahydrofuranylurethane-containing nonpeptidic protease inhibitor (PI) UIC-94017 (TMC114) with potent activity against multi-PI-resistant human immunodeficiency virus in vitro. Antimicrob. Agents Chemother. **47:**3123–3129.
21. **Kosalaraksa, P., M. F. Kavlick, V. Maroun, R. Le, and H. Mitsuya.** 1999. Comparative fitness of multi-dideoxynucleoside-resistant human immunodeficiency virus type 1 (HIV-1) in an in vitro competitive HIV-1 replication assay. J. Virol. **73:**5356–5363.
22. **Kuiken, C., B. Foley, P. Marx, S. Wolinsky, T. Leitner, B. Hahn, F. McCuthan, and B. Korber.** 2008. HIV sequence compendium 2008. LA-UR 08-03719. Theoretical Biology and Biophysics Group, Los Alamos National Laboratory, Los Alamos, NM.
23. **Larder, B. A., S. D. Kemp, and P. R. Harrigan.** 1995. Potential mechanism for sustained antiretroviral efficacy of AZT-3TC combination therapy. Science **269:**696–699.
24. **Maeda, K., K. Yoshimura, S. Shibayama, H. Habashita, H. Tada, K. Sagawa, T. Miyakawa, M. Aoki, D. Fukushima, and H. Mitsuya.** 2001. Novel low molecular weight spirodiketopiperazine derivatives potently inhibit R5 HIV-1 infection through their antagonistic effects on CCR5. J. Biol. Chem. **276:**35194–35200.
25. **Maguire, M. F., R. Guinea, P. Griffin, S. Macmanus, R. C. Elston, J. Wolfram, N. Richards, M. H. Hanlon, D. J. Porter, T. Wrin, N. Parkin, M. Tisdale, E. Furfine, C. Petropoulos, B. W. Snowden, and J. P. Kleim.** 2002. Changes in human immunodeficiency virus type 1 Gag at positions L449 and P453 are linked to I50V protease mutants in vivo and cause reduction of sensitivity to amprenavir and improved viral fitness in vitro. J. Virol. **76:**7398–7406.
26. **Mammano, F., C. Petit, and F. Clavel.** 1998. Resistance-associated loss of viral fitness in human immunodeficiency virus type 1: phenotypic analysis of protease and gag coevolution in protease inhibitor-treated patients. J. Virol. **72:**7632–7637.
27. **Mitsuya, H., and J. W. Erickson.** 1999. Discovery and development of antiretroviral therapeutics for HIV infection, p. 751–780. *In* T. C. Merigan, J. G. Bartlet, and D. Bolognes (ed.), Textbook of AIDS medicine. The Williams & Wilkins Co., Baltimore, MD.
28. **Murphy, E. L., A. C. Collier, L. A. Kalish, S. F. Assmann, M. F. Para, T. P. Flanigan, P. N. Kumar, L. Mintz, F. R. Wallach, and G. J. Nemo.** 2001. Highly active antiretroviral therapy decreases mortality and morbidity in patients with advanced HIV disease. Ann. Intern. Med. **135:**17–26.
29. **Nijhuis, M., N. M. van Maarseveen, S. Lastere, P. Schipper, E. Coakley, B. Glass, M. Rovenska, D. de Jong, C. Chappey, I. W. Goedegebuure, G. Heilek-Snyder, D. Dulude, N. Cammack, L. Brakier-Gingras, J. Konvalinka, N. Parkin, H. G. Krausslich, F. Brun-Vezinet, and C. A. Boucher.** 2007. A novel substrate-based HIV-1 protease inhibitor drug resistance mechanism. PLoS Med. **4:**e36.
30. **Paredes, R., A. Mocroft, O. Kirk, A. Lazzarin, S. E. Barton, J. van Lunzen, T. L. Katzenstein, F. Antunes, J. D. Lundgren, and B. Clotet.** 2000. Predictors of virological success and ensuing failure in HIV-positive patients starting highly active antiretroviral therapy in Europe: results from the EuroSIDA study. Arch. Intern. Med. **160:**1123–1132.
31. **Perrin, V., and F. Mammano.** 2003. Parameters driving the selection of nelfinavir-resistant human immunodeficiency virus type 1 variants. J. Virol. **77:**10172–10175.
32. **Peters, S., M. Munoz, S. Yerly, V. Sanchez-Merino, C. Lopez-Galindez, L. Perrin, B. Larder, D. Cmarko, S. Fakan, P. Meylan, and A. Telenti.** 2001. Resistance to nucleoside analog reverse transcriptase inhibitors mediated by human immunodeficiency virus type 1 p6 protein. J. Virol. **75:**9644–9653.
33. **Resch, W., R. Ziermann, N. Parkin, A. Gamarnik, and R. Swanstrom.** 2002. Nelfinavir-resistant, amprenavir-hypersusceptible strains of human immunodeficiency virus type 1 carrying an N88S mutation in protease have reduced infectivity, reduced replication capacity, and reduced fitness and process the Gag polyprotein precursor aberrantly. J. Virol. **76:**8659–8666.
34. **Saad, J. S., S. D. Ablan, R. H. Ghanam, A. Kim, K. Andrews, K. Nagashima, F. Soheilian, E. O. Freed, and M. F. Summers.** 2008. Structure of the myristylated human immunodeficiency virus type 2 matrix protein and the role of phosphatidylinositol-(4,5)-bisphosphate in membrane targeting. J. Mol. Biol. **382:**434–447.
35. **Steinkasserer, A., R. Harrison, A. Billich, F. Hammerschmid, G. Werner, B.**

Wolff, P. Peichl, G. Palfi, W. Schnitzel, E. Mlynar, et al. 1995. Mode of action of SDZ NIM 811, a nonimmunosuppressive cyclosporin A analog with activity against human immunodeficiency virus type 1 (HIV-1): interference with early and late events in HIV-1 replication. J. Virol. **69:**814–824.

36. **Tamiya, S., S. Mardy, M. F. Kavlick, K. Yoshimura, and H. Mistuya.** 2004. Amino acid insertions near Gag cleavage sites restore the otherwise compromised replication of human immunodeficiency virus type 1 variants resistant to protease inhibitors. J. Virol. **78:**12030–12040.
37. **Tisdale, M., S. D. Kemp, N. R. Parry, and B. A. Larder.** 1993. Rapid in vitro selection of human immunodeficiency virus type 1 resistant to 3′-thiacytidine inhibitors due to a mutation in the YMDD region of reverse transcriptase. Proc. Natl. Acad. Sci. USA **90:**5653–5656.
38. **Towers, G. J., T. Hatziioannou, S. Cowan, S. P. Goff, J. Luban, and P. D. Bieniasz.** 2003. Cyclophilin A modulates the sensitivity of HIV-1 to host restriction factors. Nat. Med. **9:**1138–1143.
39. **Turner, B. G., and M. F. Summers.** 1999. Structural biology of HIV. J. Mol. Biol. **285:**1–32.
40. **Verheyen, J., E. Litau, T. Sing, M. Daumer, M. Balduin, M. Oette, G. Fatkenheuer, J. K. Rockstroh, U. Schuldenzucker, D. Hoffmann, H. Pfister, and R. Kaiser.** 2006. Compensatory mutations at the HIV cleavage sites p7/p1 and p1/p6-gag in therapy-naive and therapy-experienced patients. Antivir. Ther. **11:**879–887.
41. **Verli, H., A. Calazans, R. Brindeiro, A. Tanuri, and J. A. Guimaraes.** 2007. Molecular dynamics analysis of HIV-1 matrix protein: clarifying differences between crystallographic and solution structures. J. Mol. Graph. Model. **26:**62–68.
42. **Walensky, R. P., A. D. Paltiel, E. Losina, L. M. Mercincavage, B. R. Schackman, P. E. Sax, M. C. Weinstein, and K. A. Freedberg.** 2006. The survival benefits of AIDS treatment in the United States. J. Infect. Dis. **194:**11–19.
43. **Watkins, T., W. Resch, D. Irlbeck, and R. Swanstrom.** 2003. Selection of high-level resistance to human immunodeficiency virus type 1 protease inhibitors. Antimicrob. Agents Chemother. **47:**759–769.
44. **Yoshimura, K., R. Kato, M. F. Kavlick, A. Nguyen, V. Maroun, K. Maeda, K. A. Hussain, A. K. Ghosh, S. V. Gulnik, J. W. Erickson, and H. Mitsuya.** 2002. A potent human immunodeficiency virus type 1 protease inhibitor, UIC-94003 (TMC-126), and selection of a novel (A28S) mutation in the protease active site. J. Virol. **76:**1349–1358.
45. **Yoshimura, K., R. Kato, K. Yusa, M. F. Kavlick, V. Maroun, A. Nguyen, T. Mimoto, T. Ueno, M. Shintani, J. Falloon, H. Masur, H. Hayashi, J. Erickson, and H. Mitsuya.** 1999. JE-2147: a dipeptide protease inhibitor (PI) that potently inhibits multi-PI-resistant HIV-1. Proc. Natl. Acad. Sci. USA **96:**8675–8680.
46. **Zachary, K. C., G. J. Hanna, and R. T. D'Aquila.** 2001. Human immunodeficiency virus type 1 hypersusceptibility to amprenavir in vitro can be associated with virus load response to treatment in vivo. Clin. Infect. Dis. **33:**2075–2077.
47. **Zennou, V., F. Mammano, S. Paulous, D. Mathez, and F. Clavel.** 1998. Loss of viral fitness associated with multiple Gag and Gag-Pol processing defects in human immunodeficiency virus type 1 variants selected for resistance to protease inhibitors in vivo. J. Virol. **72:**3300–3306.
48. **Zhang, Y. M., H. Imamichi, T. Imamichi, H. C. Lane, J. Falloon, M. B. Vasudevachari, and N. P. Salzman.** 1997. Drug resistance during indinavir therapy is caused by mutations in the protease gene and in its Gag substrate cleavage sites. J. Virol. **71:**6662–6670.
49. **Ziermann, R., K. Limoli, K. Das, E. Arnold, C. J. Petropoulos, and N. T. Parkin.** 2000. A mutation in human immunodeficiency virus type 1 protease, N88S, that causes in vitro hypersensitivity to amprenavir. J. Virol. **74:**4414–4419.

Antiviral Research 83 (2009) 201–204

Contents lists available at ScienceDirect

Antiviral Research

journal homepage: www.elsevier.com/locate/antiviral

Short communication

Inhibition of porcine endogenous retrovirus (PERV) replication by HIV-1 gene expression inhibitors

Minyi Shi[a,b,1], Xin Wang[b,2], Mika Okamoto[b], Sonshin Takao[a], Masanori Baba[b,*]

[a] Frontier Science Research Center, Kagoshima University, Kagoshima 890-8544, Japan
[b] Division of Antiviral Chemotherapy, Center for Chronic Viral Diseases, Graduate School of Medical and Dental Sciences, Kagoshima University, Kagoshima 890-8544, Japan

ARTICLE INFO

Article history:
Received 11 March 2009
Received in revised form 14 April 2009
Accepted 28 April 2009

Keywords:
Xenotransplantation
PERV
HIV-1
Gene expression
Chemotherapy

ABSTRACT

Porcine endogenous retrovirus (PERV) is persistently integrated into the host genomic DNA as a provirus and released from a variety of porcine cells. PERV infects a certain range of human cells, which is a major concern in xenotransplantation. Therefore, the use of viral gene expression inhibitors could be envisaged, if they reduce PERV production from porcine organs and minimize viral transmission to human recipients. In the present study, four HIV-1 gene expression inhibitors were examined for their inhibitory effect on PERV replication in porcine cells constitutively producing the virus. Among the compounds, the fluoroquinolone derivative K-37 and the bacterial product EM2487 displayed potent and selective inhibition of PERV replication in the cells mediated by the suppression of viral mRNA synthesis. Thus, retroviral gene expression inhibitors may be able to reduce the risk of PERV transmission.

Xenotransplantation, the grafting of cells, tissues, or organs into different species, is a possible solution to overcome the extreme shortage of human allografts for transplantation (Cooper and Keogh, 2001). Among the animals, non-human primates and pigs are considered to be suitable donors for xenotransplantation. The use of non-human primates as organ donors is associated with a high risk of transmitting various infectious pathogens to humans (Allan, 2003). Apart from immunological rejection, pigs may be more suitable donors than non-human primates because of the resemblance of their organ sizes and a lower risk of transmitting various infectious pathogens. However, porcine endogenous retrovirus (PERV) is still a major obstacle to successful xenotransplantation with sufficient safety. PERV is a type C retrovirus persistently integrated into the host genomic DNA as a provirus. Multiple copies of PERV proviral DNA exist in all of the breeds examined to date (Louz et al., 2008). PERV is classified into three subtypes, such as PERV-A, -B, and -C, based on the divergence of its envelope genes.

It has been demonstrated that PERV particles are released from a variety of porcine cells and infect a certain range of human cells (Martin et al., 1998; Patience et al., 1997; Wilson et al., 1998). There are a number of patients who received porcine tissues, such as pancreatic islet cells, skin, liver, and kidney; nevertheless PERV infection has not been observed in these individuals (Heneine et al., 1998; Paradis et al., 1999; Patience et al., 1998). However, long-lived microchimerism was found in some patients treated by extracorporeal splenic perfusion, which might increase a potential risk of PERV infection through the activation of viral replication (Paradis et al., 1999). An immunosuppressive treatment upon organ transplantation may also increase a risk of PERV transmission. The use of antiretrovirals would be the first option to minimize the possibility of PERV transmission to recipients, if they could have an inhibitory effect on PERV replication without serious side effects. Among the antiretrovirals, zidovudine (AZT) and didanosine (ddI) proved to be active against PERV replication in cell cultures (Powell et al., 2000; Qari et al., 2001). We have previously demonstrated that the acyclic nucleoside phosphonate tenofovir (PMPA), an HIV-1 reverse transcriptase (RT) inhibitor, selectively inhibits PERV replication in human cells (Shi et al., 2007). However, such RT inhibitors cannot suppress the production of PERV from the porcine cells in which its proviral DNA is integrated. Therefore, it would be very useful if an inhibitor of PERV gene expression could be identified. In the present study, we have examined four inhibitors of HIV-1 gene expression for their antiviral activity against PERV replication in porcine cells persistently infected with the virus and found that the fluoroquinolone derivative K-37 (Baba et al., 1998) and the bacterial product EM2487 (Baba et al., 1999) are potent and selective inhibitors of PERV replication.

K-37 and the nuclear factor κB (NF-κB) inhibitor cepharanthine (Okamoto et al., 1998) were provided by Daiichi Pharmaceutical

* Corresponding author. Tel.: +81 99 275 5930; fax: +81 99 275 5932.
E-mail address: m-baba@vanilla.ocn.ne.jp (M. Baba).
[1] Present address: Department of Molecular, Cellular, and Developmental Biology, Yale University, New Haven, CT 06520, USA.
[2] Present address: Department of Pharmacology, Yale University School of Medicine, New Haven, CT 06520, USA.

0166-3542/$ – see front matter © 2009 Elsevier B.V. All rights reserved.
doi:10.1016/j.antiviral.2009.04.011

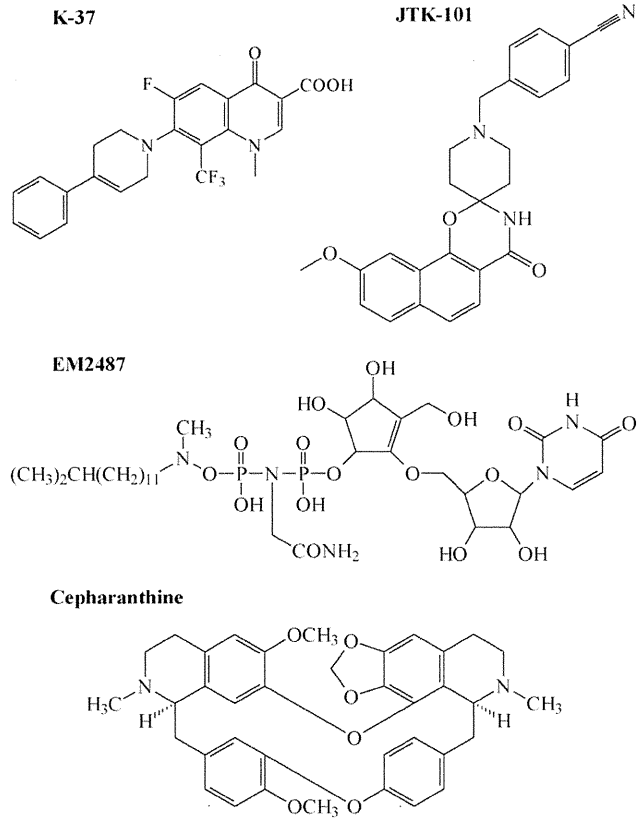

Fig. 1. Chemical structures of test compounds.

Co. (Tokyo, Japan) and Kaken Shoyaku (Mitaka, Japan), respectively. JTK-101 (Wang et al., 2007) was synthesized by Japan Tobacco Co. (Takatsuki, Japan). EM2487 was provided by Esai Co. (Tsukuba, Japan). These compounds (Fig. 1) were chosen for this study, because their antiviral activity against HIV-1 replication in chronically infected cells had been demonstrated (Baba et al., 1998, 1999; Okamoto et al., 1998; Wang et al., 2007). All compounds were dissolved in dimethyl sulfoxide (DMSO) at 10 mM or higher concentrations to exclude any antiviral or cytotoxic effect of DMSO and stored −20 °C until use. The porcine embryonic kidney cell line PK15, which produces PERV particles, was obtained from the American Type Culture Collection. The cells were maintained in Eagle's minimal essential medium supplemented with 10% fetal bovine serum, 0.1 mM nonessential amino acids, 1 mM sodium pyruvate, 1.5 g/l sodium bicarbonate, and antibiotics.

The activity of the compounds against persistent PERV infection was based on the inhibition of PERV particle production from PK15 cells. PK15 cells were seeded in a 24-well plate (2.5×10^4 cells/well). After incubation for 16 h at 37 °C, the culture supernatants were removed and the cell monolayer was washed by phosphate-buffered saline (PBS), and then 2 ml of fresh medium containing various concentrations of the test compounds was added to each well. After a 48-h incubation period, the culture supernatants were collected and filtered (0.45 μm pore size). Then the filtrates were mixed with 22% (w/v) polyethylene glycol 6000 solution. After incubation for 5 h at 4 °C with continuous stirring, the mixture was centrifuged at 15,000 rpm for 15 min at 4 °C. The pellets contained PERV particles released from PK15 cells. The inhibition of PERV particle production was determined by the decrease of PERV reverse transcriptase activity using a commercial RT assay kit (Roche, Mannheim, Germany). The pellets obtained above were resuspended in lysis buffer supplied by the assay kit and subjected to reverse transcription reaction for 2 h, according to the Manufacturer's instructions, except that $MgCl_2$ in the reaction mixture was replaced by $MnCl_2$ (Phan-Thanh et al., 1992). All experiments were carried out in duplicate.

The antiviral activity of test compounds was also determined by the inhibition of PERV mRNA expression in PK15 cells. PK15 cells were seeded and cultured in the medium containing test compounds in the same manner as described for the antiviral assay. After a 48-h incubation, the culture supernatants were removed, and the cells were extensively washed with PBS, trypsinized, and washed again with PBS. Total RNA was extracted from the cells with RNeasy Mini Kit (Qiagen) and subjected to real-time RT-PCR analysis. The PERV mRNA level was determined using the sense primer (5′-AGCTCCGGGAGGCCTACTC-3′), the antisense primer (5′-ACAGCCGTTGGTGTGGTCA-3′), and the Taqman® probe (5′-FAM-CCACCGTGCAGGAAACCTCGAGACT-TAMRA-3′). The primer pair amplifies a region of the *pol* gene of PERV (Paradis et al., 1999). The nucleotide sequences used for the construction of the primers and probe were based on the reports by B. Bartosch, R.A. Weiss and Y. Takeuchi (GeneBank accession numbers: AY099323 and AY099324). The final concentrations of the primer pairs and probe were 200 and 100 nM, respectively. The Taqman® PCR reagent kit and Taqman® Multiscribe™ reverse transcription reagent kit (Applied Biosystems, Roche, Branchburg, NJ) were used according to the Manufacturer's instructions. Each sample was run in triplicate. Nonspecific inhibition of host cellular mRNA synthesis by the test compounds was determined with the Taqman 18S rRNA reagent kit (Applied Biosystems).

Cytotoxicity of the test compounds was determined by a tetrazolium dye method (Tetracolor One®, Seikagaku Corporation, Tokyo, Japan) (Yamamoto et al., 2001). PK15 cells were seeded and cultured in the medium containing test compounds in the same manner, as described in the antiviral assay. After a 48-h incubation, 1.5 ml of the culture supernatants were removed and 25 μl of the dye was added to each well. After a 4-h incubation at 37 °C, the specific (450 nm) and reference (630 nm) absorbances were monitored for each well by a microplate reader.

When four HIV-1 gene expression inhibitors were examined for their inhibitory effect on PERV replication in PK15 cells, K-37 and EM2487 displayed dose-dependent reduction of PERV RT activity in culture supernatants (Fig. 2A and C). K-37 and EM2487 did not show a direct inhibitory effect on PERV RT activity (data not shown). These compounds did not display apparent cytotoxicity to PK15 cells at concentrations up to 1 and 10 μM, respectively, indicating that K-37 and EM2487 are selective inhibitors of PERV replication in porcine cells. In contrast, JTK-101 and cepharanthine did not show any activity against PERV replication at the highest concentration tested (1 μM) (Fig. 2B and D). Since PERV proviral DNA is integrated in the genome of the host cells, the compounds were also examined for their inhibitory effect on viral mRNA synthesis in PK15 cells. As shown in Fig. 3, dose-dependent suppression of PERV mRNA synthesis was observed for K-37 and EM2487 but not for JTK-101 or cepharanthine. These results are in accordance with those obtained in the RT assay (Fig. 2). The 50% effective concentration (EC_{50}) of K-37 for PERV replication and its 50% inhibitory concentration (IC_{50}) for viral mRNA synthesis were 0.35 ± 0.04 and 0.34 ± 0.05 μM, respectively (Table 1). On the other hand, its 50% cytotoxic concentration (CC_{50}) was 4.63 ± 1.62 μM, suggesting that K-37 is a selective inhibitor of PERV gene expression. Similarly, the EC_{50}, IC_{50}, and CC_{50} of EM2487 were 5.44 ± 1.40, 4.36 ± 0.30, and >10 μM, respectively.

K-37 is a potent and selective inhibitor of HIV-1 replication in both acutely and chronically infected cells at submicromolar concentrations (Baba et al., 1998). K-37 could inhibit Tat-dependent transactivation, yet it was not an inhibitor of Tat itself or its cofactor CDK9/cyclin T1. Since PERV does not generate Tat protein, it is apparent that the anti-PERV activity of K-37 is not due to the inhi-

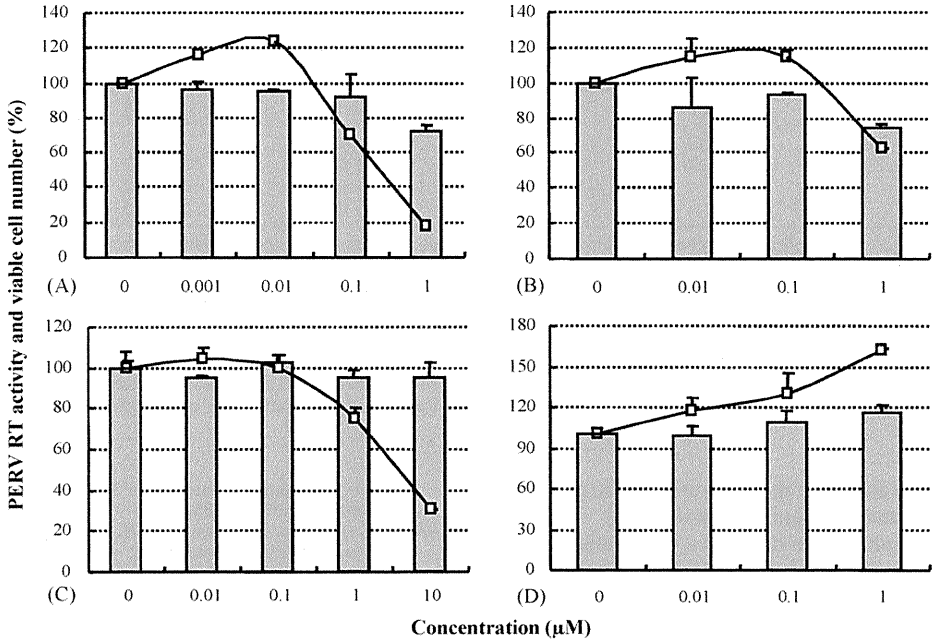

Fig. 2. Inhibitory effects of the test compounds on PERV replication in PK15 cells. PK15 cells were cultured in the presence of various concentrations of (A) K-37, (B) JTK-101, (C) EM2487 and (D) cepharanthine. After a 48-h incubation period, the culture supernatants were collected and mixed with 22% (w/v) polyethylene glycol 6000 solution for 5 h. PERV particles were harvested by centrifugation of the mixture. The viral pellets were resuspended in lysis buffer and subjected to RT assay (lines). The viable cell number was determined by a tetrazolium dye cell proliferation assay (bars). Both the RT activity and cell proliferation assays were performed in duplicate. The data represent means plus ranges. Representative results for two independent experiments are shown.

bition of Tat functions. Furthermore, K-37 was reported to inhibit the gene expression of human T-lymphotropic virus type 1 (HTLV-1) in persistently infected cells (Wang et al., 2002a). Although the target molecule of K-37 still remains to be determined, the present observations for PERV suggest that K-37 may interact with a cellular factor or factors that play an important role in retroviral gene expression. It is assumed that K-37 inhibits an early stage of transcriptional elongation of viral RNA (Okamoto et al., unpublished observations). EM2487 is a substance produced from a *Streptomyces* species and a potent and selective inhibitor of HIV-1 replication in acutely and chronically infected cells (Baba et al., 1999). Like K-37, EM2487 could inhibit HTLV-1 gene expression without affecting host cellular functions (Wang et al., 2002b). The chemical structures of K-37 and EM2487 are totally different from each other

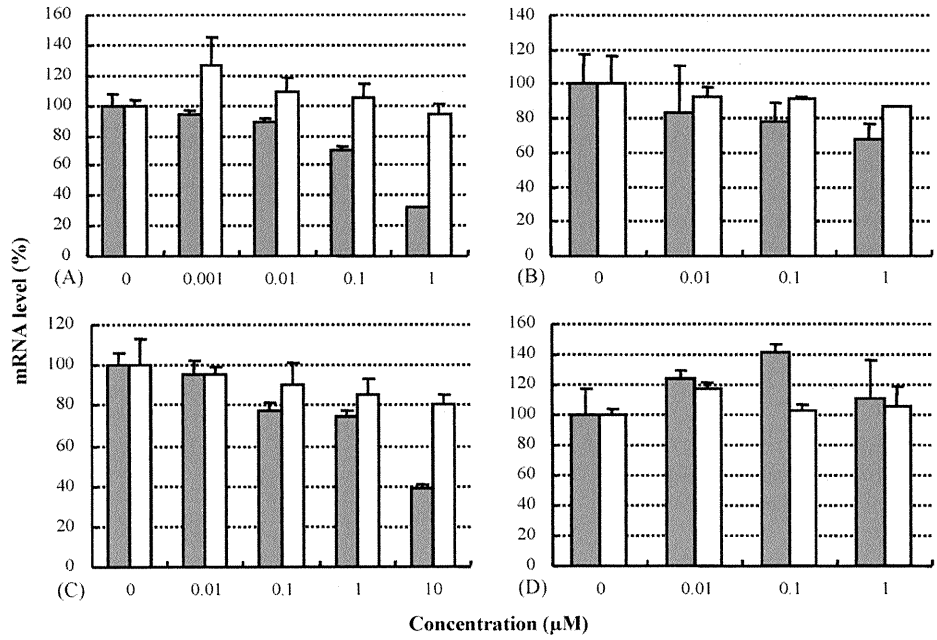

Fig. 3. Inhibitory effect of the test compounds on PERV mRNA synthesis in PK15 cells. PK15 cells were cultured in the presence of various concentrations of (A) K-37, (B) JTK-101, (C) EM2487 and (D) cepharanthine. After a 48-h incubation, the cells were collected, and total RNA was extracted. Quantitative real-time RT-PCR was performed to determine the amount of PERV mRNA in PK15 cells using a primer pair and probe specific to the PERV *pol* gene (gray columns). The inhibitory effect of the test compounds on host cellular mRNA synthesis was determined by quantitative RT-PCR for 18S mRNA (white columns). All experiments were performed in triplicate. The data represent means plus standard deviations. Representative results for two independent experiments are shown.

Table 1
Inhibitory effect of test compounds on PERV antigen production and mRNA synthesis in PK15 cells[a].

Compounds	PERV[b]			HIV-1[c]		HTLV-1[d]	
	EC_{50} (μM)	IC_{50} (μM)	CC_{50} (μM)	EC_{50} (μM)	CC_{50} (μM)	EC_{50} (μM)	CC_{50} (μM)
K-37	0.35 ± 0.04	0.34 ± 0.05	4.63 ± 1.62	0.033 ± 0.012	2.1 ± 0.3	0.44 ± 0.13	5.7 ± 1.0
EM2487	5.44 ± 1.40	4.36 ± 0.30	>10	0.075 ± 0.032	12.5 ± 4.1	3.6 ± 0.6	30.6 ± 3.5
JTK-101	>1	>1	2.18 ± 0.63	0.0014 ± 0.0005	3.8 ± 0.2	N.D.[e]	N.D.
Cepharanthine	>1	>1	4.39 ± 1.99	0.028 ± 0.016	1.3 ± 0.3	>3.0	3.0 ± 0.4

[a] Each experiment was carried out in duplicate or triplicate, and all data represent means ± ranges for two independent experiments.

[b] EC_{50}: 50% effective concentration based on the inhibition of PERV antigen production (RT) in culture supernatants of PK15 cells. IC_{50}: 50% inhibitory concentration based on the inhibition of PERV mRNA synthesis. CC_{50}: 50% cytotoxic concentration based on the inhibition of host cell proliferation.

[c] EC_{50}: 50% effective concentration based on the inhibition of HIV-1 antigen production (p24) in chronically infected cells. CC_{50}: 50% cytotoxic concentration based on the inhibition of host cell proliferation. Data are taken from the reports by Wang et al. (2007) for K-37 and JTK-101, Baba et al. (1999) for EM2487, and Baba et al. (2001) for cepharanthine.

[d] EC_{50}: 50% effective concentration based on the inhibition of HTLV-1 antigen production (p19) in infected cells. CC_{50}: 50% cytotoxic concentration based on the inhibition of host cell proliferation. Data are taken from the reports by Wang et al. (2002a) for K-37 and cepharanthine and Wang et al. (2002b) for EM2487.

[e] Not determined.

(Fig. 1), nevertheless they appear to share some common properties in antiretroviral activity and mechanism of action.

JTK-101 is a novel naphthalene derivative that inhibits HIV-1 replication in cell cultures (Wang et al., 2007). This compound was found to be highly active against HIV-1 in chronically infected cells but much less active in acutely infected cells. Studies of its mechanism of action suggested that JTK-101 exerted its anti-HIV-1 activity through the inhibition of CDK9/cyclin T1. Cepharantine is a plant alkaloid that has been shown to inhibit HIV-1 replication in a certain chronically infected cell line at low concentrations through the inhibition of NF-κB (Okamoto et al., 1998). Cepharanthine could also suppress stimulation-induced production of proinflammatory cytokines in human macrophages (Okamoto et al., 2001). This compound did not inhibit PERV replication in PK15 cells or even slightly enhanced it at the highest concentration tested (Fig. 2D).

The viral gene expression inhibitors K-37 and EM2487 may be able to keep PERV silent in porcine organs thereby reducing the risk of PERV transmission to recipients, which is never attainable with RT inhibitors. On the other hand, RT inhibitors are capable of inhibiting De Novo infection of recipients with PERV derived from porcine organs. Thus, an ideal strategy to prevent PERV transmission to organ recipients may be the combined treatment with an RT inhibitor for recipients and a gene expression inhibitor for donor organs. Unfortunately, the current gene expression inhibitors, such as K-37 or EM2487, may be toxic to human recipients at concentrations that completely suppress PERV production from donor cells or organs. Therefore, the optimization of their chemical structures would be required for the inhibition of PERV replication in vivo without generating serious side effects. Although the risk of PERV transmission upon xenotransplantation is supposed to be lower than initially thought, optimized retroviral gene expression inhibitors may be worth further pursuing for their potential efficacy in the clinical setting.

Acknowledgments

This work was supported in part by a Grant-in-Aid for Scientific Research (S) (grant no. 17100007) from the Ministry of Education, Science, Sports, Culture and Technology of Japan.

References

Allan, J.S., 2003. Understanding xenotransplantation risks from nonhuman primate retroviruses. Curr. Top. Microbiol. Immunol. 278, 101–123.

Baba, M., Okamoto, M., Kawamura, M., Makino, M., Higashida, T., Takashi, T., Kimura, Y., Ikeuchi, T., Tetsuka, T., Okamoto, T., 1998. Inhibition of human immunodeficiency virus type 1 replication and cytokine production by fluoroquinoline derivatives. Mol. Pharmacol. 53, 1097–1103.

Baba, M., Okamoto, M., Takeuchi, T., 1999. Inhibition of human immunodeficiency virus type 1 replication in acutely and chronically infected cells by EM2487, a novel substance produced by a *Streptomyces* species. Antimicrob. Agents Chemother. 43, 2350–2355.

Baba, M., Okamoto, M., Kashiwaba, N., Ono, M., 2001. Anti-HIV-1 activity and structure–activity relationship of cepharanoline derivatives in chronically infected cells. Antiviral Chem. Chemother. 12, 307–312.

Cooper, D.K., Keogh, A.M., 2001. The potential role of xenotransplantation in treating endstage cardiac disease: a summary of the report of the Xenotransplantation Advisory Committee of the International Society for Heart and Lung Transplantation. Curr. Opin. Cardiol. 16, 105–109.

Heneine, W., Tibell, A., Switzer, W.M., Sandstrom, P., Rosales, G.V., Mathews, A., Korsgren, O., Chapman, L.E., Folks, T.M., Groth, C.G., 1998. No evidence of infection with porcine endogenous retrovirus in recipients of porcine islet-cell xenografts. Lancet 352, 695–699.

Louz, D., Bergmans, H.E., Loos, B.P., Hoeben, R.C., 2008. Reappraisal of biosafety risks posed by PERVs in xenotransplantation. Rev. Med. Virol. 18, 53–65.

Martin, U., Kiessig, V., Blusch, J.H., Haverich, A., von der Helm, K., Herden, T., Steinhoff, G., 1998. Expression of pig endogenous retrovirus by primary porcine endothelial cells and infection of human cells. Lancet 352, 692–694.

Okamoto, M., Ono, M., Baba, M., 1998. Potent inhibition of HIV type 1 replication by an anti-inflammatory alkaloid, cepharanthine, in chronically infected monocytic cells. AIDS Res. Hum. Retroviruses 14, 1239–1245.

Okamoto, M., Ono, M., Baba, M., 2001. Suppression of cytokine production and neural cell death by the anti-inflammatory alkaloid cepharanthine: a potential agent against HIV-1 encephalopathy. Biochem. Pharmacol. 62, 747–753.

Patience, C., Patton, G.S., Takeuchi, Y., Weiss, R.A., McClure, M.O., Rydberg, L., Breimer, M.E., 1998. No evidence of pig DNA or retroviral infection in patients with short-term extracorporeal connection to pig kidneys. Lancet 352, 699–701.

Patience, C., Takeuchi, Y., Weiss, R.A., 1997. Infection of human cells by an endogenous retrovirus of pigs. Nat. Med. 3, 282–286.

Paradis, K., Langford, G., Long, Z., Heneine, W., Sandstrom, P., Switzer, W.M., Chapman, L.E., Lockey, C., Onions, D., Otto, E., The XEN 111 Study Group, 1999. Search for cross-species transmission of porcine endogenous retrovirus in patients treated with living pig tissue. Science 285, 1236–1241.

Phan-Thanh, L., Kaeffer, B., Bottreau, E., 1992. Porcine retrovirus: optimal conditions for its biochemical detection. Arch. Virol. 123, 255–265.

Powell, S.K., Gates, M.E., Langford, G., Gu, M.-L., Lockey, C., Long, Z., Otto, E., 2000. Antiretroviral agents inhibit infection of human cells by porcine endogenous retroviruses. Antimicrob. Agents Chemother. 44, 3432–3433.

Qari, S.H., Magre, S., Garcia-Lerma, J.G., Hussain, A.I., Takeuchi, Y., Patience, C., Weiss, R.A., Heneine, W., 2001. Susceptibility of the porcine endogenous retrovirus to reverse transcriptase and protease inhibitors. J. Virol. 75, 1048–1053.

Shi, M., Wang, X., De Clercq, E., Takao, S., Baba, M., 2007. Selective inhibition of porcine endogenous retrovirus replication in human cells by acyclic nucleoside phosphonates. Antimicrob. Agents Chemother. 51, 2600–2604.

Wang, X., Miyake, H., Okamoto, M., Saito, M., Fujisawa, J., Tanaka, Y., Izumo, S., Baba, M., 2002a. Inhibition of the tax-dependent human T-lymphotropic virus type I replication in persistently infected cells by the fluoroquinolone derivative k-37. Mol. Pharmacol. 61, 1359–1365.

Wang, X., Okamoto, M., Kawamura, M., Izumo, S., Baba, M., 2002b. Inhibition of human T-lymphotropic virus type I gene expression by the Streptomyces-derived substance EM2487. Antiviral Chem. Chemother. 13, 177–183.

Wang, X., Yamataka, K., Okamoto, M., Ikeda, S., Baba, M., 2007. Potent and selective inhibition of Tat-dependent HIV-1 replication in chronically infected cells by a novel naphtalene derivative JTK-101. Antiviral Chem. Chemother. 18, 201–211.

Wilson, C.A., Wong, S., Muller, J., Davidson, C.E., Rose, T.M., Burd, P., 1998. Type C retrovirus released from porcine primary peripheral blood mononuclear cells infects human cells. J. Virol. 72, 3082–3087.

Yamamoto, O., Hamada, T., Tokui, N., Sasaguri, Y., 2001. Comparison of three in vitro assay systems used for assessing cytotoxic effect of heavy metals on cultured human keratinocytes. J. UOEH 23, 35–44.

THE JOURNAL OF BIOLOGICAL CHEMISTRY VOL. 284, NO. 8, pp. 4914–4920, February 20, 2009

Design of Peptide-based Inhibitors for Human Immunodeficiency Virus Type 1 Strains Resistant to T-20*[S]

Received for publication, September 16, 2008, and in revised form, December 3, 2008 Published, JBC Papers in Press, December 10, 2008, DOI 10.1074/jbc.M807169200

Kazuki Izumi[‡], Eiichi Kodama[‡1], Kazuya Shimura[‡], Yasuko Sakagami[‡], Kentaro Watanabe[§], Saori Ito[§], Tsuyoshi Watabe[§], Yukihiro Terakawa[§], Hiroki Nishikawa[§], Stefan G. Sarafianos[¶], Kazuo Kitaura[§], Shinya Oishi[§], Nobutaka Fujii[§], and Masao Matsuoka[‡]

From the [‡]Institute for Virus Research, Kyoto University, 53 Kawaramachi, Shogoin, Kyoto 606-8507, Japan, the [§]Graduate School of Pharmaceutical Sciences, Kyoto University, 46-29 Yoshida, Shimoadachi-cho, Kyoto 606-8501, Japan, and the [¶]Christopher S. Bond Life Sciences Center and Department of Molecular Microbiology and Immunology, University of Missouri School of Medicine, Columbia, Missouri 65211

Enfuvirtide (T-20) is a fusion inhibitor that suppresses replication of human immunodeficiency virus (HIV) variants with multi-drug resistance to reverse transcriptase and protease inhibitors. It is a peptide derived from the C-terminal heptad repeat (C-HR) of HIV-1 gp41, and it prevents interactions between the C-HR and the N-terminal HR (N-HR) of gp41, thus interfering with conformational changes that are required for viral fusion. However, prolonged therapies with T-20 result in the emergence of T-20-resistant strains that contain primary mutations such as N43D in the N-HR of gp41 (where T-20 and C-HR bind) that help the virus escape at a fitness cost. Such variants often go on to acquire a secondary mutation, S138A, in the C-HR of gp41 region that corresponds to the sequence of T-20. We demonstrate here that the role of S138A is to compensate for the impaired fusion kinetics of HIV-1s carrying primary mutations that abrogate binding of T-20. To preempt this escape strategy, we designed a modified T-20 variant containing the S138A substitution and showed that it is a potent inhibitor of both T-20-sensitive and T-20-resistant viruses. Circular dichroism analysis revealed that the S138A provided increased stability of the 6-helix bundle. We validated our approach on another fusion inhibitor, C34. In this case, we designed a variant of C34 with the secondary escape mutation N126K and showed that it can effectively inhibit replication of C34-resistant HIV-1. These results prove that it is possible to design improved peptide-based fusion inhibitors that are efficient against a major mechanism of drug resistance.

HIV-1[2] entry into the target cells is mediated by two envelope glycoproteins, gp120 and gp41, that form a trimeric gp120·gp41 complex. After binding of gp120 to the CD4 receptor and CCR5 (or CXCR4) coreceptor on the surface of the target cell, the gp41 trimer forms an extended conformation of the three helices that allows a hydrophobic fusion peptide to be inserted into the target cell membrane, generating an intermediate that is anchored to both cellular and viral membranes. After this step, the gp41 is believed to start refolding to a more stable 6-helix bundle composed of the α-helical trimer of the N-terminal heptad repeat (N-HR) folded into an anti-parallel conformation with the three C-terminal heptad repeats (C-HR) (1, 2). This refolding brings the viral and cellular membranes together to catalyze fusion.

The transition of the extended intermediate to the 6-helix bundle can be inhibited by the addition of exogenous peptides derived from gp41 C-HR (Fig. 1*A*) that prevent the formation of the 6-helix bundle and inhibit the HIV-1 fusion with the target cells (3–6). T-20, a 36-amino acid peptide derived from C-HR, effectively suppresses *in vivo* replication of HIV-1 resistant to inhibitors of reverse transcriptase and protease (7, 8). However, HIV-1 variants resistant to T-20 have recently emerged carrying primary mutations in the Leu-33–Leu-45 region of the N-HR domain (9–15). Among them, V38A and N43D seem to be major primary mutations for T-20 resistance. Meanwhile, a secondary mutation at the C-HR region (S138A) has been reported to enhance T-20 resistance with an as yet undefined mechanism (9, 14, 15) (Fig. 1*B*).

The mechanism of resistance to C34, another C-HR peptide-based inhibitor of HIV fusion, has been the subject of multiple studies (13, 16). Because of a 22-amino acid overlap between the T-20 and C34 peptides (Fig. 1*B*), HIV-1 has developed primary mutations for C34 resistance *in vitro* at the identical Leu-33–Leu-45 region of the peptides. During *in vitro* selection of C34 resistance, we identified a mutation in the C-HR domain, N126K, that is also observed in some T-20-resistant clinical variants (10, 15, 17). We showed that N126K conferred resistance to C34 by compensating for the impaired intra-gp41 inter-

* This work was supported, in part, by National Institutes of Health Grants AI076119, AI079801, and AI074389 (to S. G. S.). This work was also supported in part by grants from the Ministry of Health and Welfare and the Ministry of Education, Culture, Sports, Science, and Technology of Japan (to E. K., S. O., and N. F.), the Japan Health Sciences Foundation (to E. K., S. O., N. F., and M. M.), the 21st Century COE program (to K. I., S. I., and H. N.), and a Japan Society for the Promotion of Science research fellowship (to H. N.). The costs of publication of this article were defrayed in part by the payment of page charges. This article must therefore be hereby marked "*advertisement*" in accordance with 18 U.S.C. Section 1734 solely to indicate this fact.

[S] The on-line version of this article (available at http://www.jbc.org) contains supplemental Figs. 1 and 2 and Tables 1 and 2.

[1] To whom correspondence should be addressed. Tel. and Fax: 81-75-751-3986; E-mail: ekodama@virus.kyoto-u.ac.jp.

[2] The abbreviations used are: HIV, human immunodeficiency virus; T-20, enfuvirtide; HR, heptad repeat; MAGI, multinuclear activation of galactosidase indicator; EC_{50}, 50% effective concentration; T_m, melting temperature; CD, circular dichroism; shRNA, short hairpin RNA; WT, wild-type.

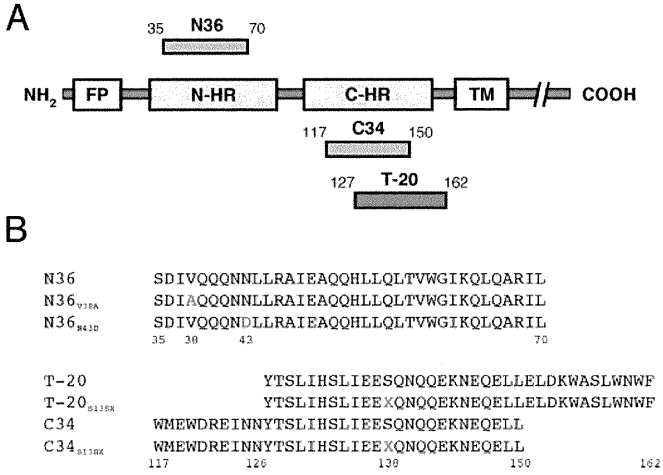

FIGURE 1. **Schematic view of gp41 and peptide sequence.** *A*, structure of HIV-1 gp41 and locations of N-HR or C-HR peptides (*FP*, fusion peptide; *TM*, transmembrane domain). *B*, amino acid sequences of peptides used in this study. Only the amino acid located at Ser-138 was substituted with all physiological amino acids (*X*), as Asn-126 lies outside of the amino acid sequence of T-20.

action by a primary mutation, I37K (13). N126K was initially identified in background of V38A, another primary mutation, for T-20 resistance *in vivo* (17). Baldwin *et al.* (17, 18) demonstrated a striking T-20-dependent replication phenotype in the V38A/N126K variant and proposed that T-20 acts as a safety pin to prevent premature formation of helical bundle, as N126K enhanced binding capacity of the introduced C-HR to N36 with V38A. Taken together, these studies suggest that mutations in the C-HR serve as secondary mutations.

In this study we show that the main role of secondary mutations that follow the appearance of primary mutations during treatment with peptide-based fusion inhibitors is to compensate for the impairment in replication kinetics that is caused by the primary mutations (supplemental Fig. 1). Based on this finding we hypothesized that analogs of T-20 carrying substitutions corresponding to secondary T-20 resistance mutations should be active against both wild-type and T-20-resistant viruses containing primary mutations. Indeed, our results confirmed our hypothesis and showed that T-20 with the S138A substitution (T-20_{S138A}) has a strong anti-HIV-1 activity even against T-20-resistant clones. Moreover, we demonstrate that this restoration is concomitant to improved binding of C-HR_{S138A} to N-HR_{N43D}, suggesting that our approach utilizing the resistance-associated mutations to design peptides may provide useful broad insights into effective peptide-based therapies.

EXPERIMENTAL PROCEDURES

Cells and Viruses—MT-2 cells were grown in RPMI 1640 medium. 293T cells were grown in Dulbecco's modified Eagle's medium-based culture medium. HeLa-CD4-LTR-β-gal cells were kindly provided by M. Emerman through the AIDS Research and Reference Reagent Program, Division of AIDS, NIAID, National Institutes of Health (Bethesda, MD) and were used for the drug susceptibility assay as described previously (13, 19, 20). An HIV-1 infectious clone, pNL4–3 (21), was used for generation of HIV-1 variants.

Antiviral Agents—The peptides used in this study were synthesized as described previously (6).

Determination of Drug Susceptibility of HIV-1—The peptide sensitivity of infectious clones was determined by the multinuclear activation of galactosidase indicator (MAGI) assay as described previously (13). Briefly, the target cells (HeLa-CD4-LTR-β-gal; 10^4 cells/well) were plated in 96-well flat microtiter culture plates. On the following day the cells were inoculated with the HIV-1 clones (60 MAGI unit/well, giving 60 blue cells after 48 h of incubation) and cultured in the presence of various concentrations of drugs in fresh medium. Forty-eight hours after viral exposure, all the blue cells stained with 5-bromo-4-chloro-3-indolyl-β-D-galactopyranoside (X-gal) were counted in each well. The activity of test compounds was determined as the concentration that blocked HIV-1 replication by 50% (50% effective concentration, (EC_{50}).

Generation of Recombinant HIV-1 Clones—Recombinant infectious HIV-1 clones, carrying various mutations, were generated as described previously (13). Each molecular clone was transfected into 293T cells with *Trans*IT® (Madison, WI). After 48 h, the supernatants were harvested and stored at −80 °C until use.

Circular Dichroism Spectroscopy—Each peptide (10 μM) was mixed with 10 mM phosphate-buffered saline, pH 7.4, and the data were collected using a Jasco spectrometer (Model J-710; Jasco, Tokyo, Japan) equipped with a thermoelectric temperature controller. The thermal stability was assessed by monitoring the change in the circular dichroism signal at 222 nm. The midpoint of the thermal unfolding transition (melting temperature, (T_m) of each complex was determined as described previously (6).

Viral Replication Kinetics Assay—MT-2 cells (10^5 cells/3 ml) were infected with each virus preparation (1000 MAGI unit) for 16 h. The infected cells were then washed and cultured in a final volume of 3 ml. The culture supernatants were harvested after infection on days 2–7, and the levels of p24 antigen were determined (22).

For each competitive HIV-1 replication assay, two infectious clones of interest that had been previously titrated were mixed and added to MT-2 cells (10^5 cells/3 ml) as described previously (13, 22) with minor modifications. To ensure that the two infectious clones being compared were of approximately equal infectivity, a fixed amount (500 MAGI unit) of one infectious clone was mixed with three different amounts (250, 500, and 1000 MAGI unit) of the other infectious clone. On day 1, one-third of the infected MT-2 cells were harvested and washed twice with phosphate-buffered saline, and the cellular DNA was extracted. The purified DNA was subjected to nested PCR and then direct DNA sequencing. The HIV-1 co-culture, which best approximated a 50:50 mixture on day 1, was further propagated. Every 3–4 days, the co-culture supernatant (100 μl) was transmitted to new uninfected MT-2 cells (5×10^5 cells/3 ml). The cells harvested at the end of each passage were subjected to direct sequencing, and the viral population change was determined.

Structure Modeling of gp41 S138A Mutant Core—The gp41 core model was built using the coordinates of crystal structure of the N36/C34 complex (23) (PDB code 1AIK). The coordi-

TABLE 1

Antiviral activity of T-20-derived peptides against T-20-resistant gp41 recombinant viruses

Anti-HIV activity was determined with the MAGI assay. The data shown are the mean values and S.D. that were obtained from the results of at least three independent experiments. Shown in parentheses are the -fold increases in resistance (increase in EC_{50} value) calculated by comparison to a reference virus. Increases of >10-fold are indicated in bold.

	EC_{50}			
	HIV-1_{WT}[a]	HIV-1_{V38A}	HIV-1_{N43D}	HIV-$1_{N43D/S138A}$
	nM			
T-20	2.4 ± 0.6	23 ± 8.2 (**9.6**)	49 ± 10 (**20**)	84 ± 16 (**35**)
Small				
T-20_{S138G}	1.3 ± 0.5 (0.5)	65 ± 8.8 (**27**)	141 ± 26 (**59**)	185 ± 68 (77)
T-20_{S138A}	0.6 ± 0.1 (0.3)	3.6 ± 1.7 (1.5)	3.5 ± 0.9 (1.5)	3.2 ± 1.0 (1.3)
Hydrophobic				
T-20_{S138V}	0.4 ± 0.2 (0.2)	31 ± 14 (**13**)	22 ± 3.5 (9.2)	23 ± 5.7 (9.6)
T-20_{S138L}	0.7 ± 0.1 (0.3)	13 ± 6 (5.4)	2.9 ± 0.7 (1.2)	2.2 ± 0.4 (0.9)
T-20_{S138I}	0.5 ± 0.1 (0.2)	4.9 ± 2 (2)	2.9 ± 0.8 (1.2)	2.4 ± 0.6 (1)
T-20_{S138M}	0.7 ± 0.2 (0.3)	4.4 ± 0.1 (1.8)	1.7 ± 0.5 (0.7)	1.2 ± 0.4 (0.5)
T-20_{S138P}	446 ± 167 (**186**)	>1000 (>**416**)	>1000 (>**416**)	>1000 (>**416**)
Nucleophilic				
T-20_{S138T}	0.9 ± 0.2 (0.4)	39 ± 8.5 (**16**)	161 ± 35 (**67**)	124 ± 43 (**52**)
Aromatic				
T-20_{S138F}	9.4 ± 2.6 (4)	203 ± 89 (**85**)	393 ± 119 (**164**)	478 ± 116 (**200**)
T-20_{S138Y}	25 ± 9 (**10**)	516 ± 223 (**215**)	>1000 (>**416**)	>1000 (>**416**)
T-20_{S138W}	29 ± 14 (**12**)	>1000 (>**416**)	>1000 (>**416**)	>1000 (>**416**)
Amide				
T-20_{S138N}	19 ± 4 (8)	>1000 (>**416**)	>1000 (>**416**)	>1000 (>**416**)
T-20_{S138Q}	34 ± 11 (**14**)	>1000 (>**416**)	>1000 (>**416**)	>1000 (>**416**)
Acidic				
T-20_{S138D}	210 ± 94 (**88**)	>1000 (>**416**)	>1000 (>**416**)	>1000 (>**416**)
T-20_{S138E}	283 ± 80 (**118**)	>1000 (>**416**)	>1000 (>**416**)	>1000 (>**416**)
Basic				
T-20_{S138H}	210 ± 85 (**88**)	>1000 (>**416**)	>1000 (>**416**)	>1000 (>**416**)
T-20_{S138K}	708 ± 145 (**295**)	>1000 (>**416**)	>1000 (>**416**)	>1000 (>**416**)
T-20_{S138R}	362 ± 114 (**150**)	>1000 (>**416**)	>1000 (>**416**)	>1000 (>**416**)

[a] To improve the replication kinetics, D36G mutation, observed in the majority of HIV-1 strains, was introduced into the NL4-3 background used in this study (reference virus).

nates of the water molecules were removed. Additionally, the hydrogen atoms were placed in optimal positions and refined by the energy minimization with the AMBER9 program (24) using the FF99 force field. Ser-138 in the gp41 core model was replaced with alanine (replacement of -OH with -H), and the positions of the hydrogen atoms were refined as described above. The S138A mutant core model (N36/$C34_{S138A}$ complex) was further optimized by the energy minimization using the FF99 force field with the restraints on each of the three residues of N and C termini and the backbone atoms. The restraint weight was 5.0 kcal/mol Å^2.

RESULTS

Effect of Amino Acid Substitutions at 138 on Antiviral Activities—We chemically synthesized peptide analogs of T-20 with all natural amino acid substitutions at the 138 position (T-20_{S138X}) and evaluated them for their ability to inhibit three major T-20-resistant clones using the MAGI assay (13) (Table 1). The results indicated that only T-20_{S138A} inhibited replication of T-20-resistant clones as efficiently as the wild-type clone. Substitution to glycine enhanced T-20 activity, but unlike T-20_{S138A}, T-20_{S138G} reduced its activity against T-20-resistant clones by ~2–3-fold as compared with the parental peptide, T-20. Substitutions to hydrophobic amino acids leucine, isoleucine, and methionine maintained their anti-HIV-1 activity; however, those to valine reduced anti-HIV-1 activity to T-20-resistant clones. The proline substitution drastically decreased the anti-HIV-1 activity of the peptide inhibitors.

Nucleophilic amino acid at position 138 of T-20 (T-20_{S138T}) showed similar profiles. Conversely, aromatic and amide substitutions reduced the anti-HIV-1 activity of T-20 against HIV-1_{WT}- and T-20-resistant clones. Other amino acid substitutions, especially acidic and basic amino acids, decreased the anti-HIV-1 inhibitory activity even against HIV-1_{WT}. These results suggest that smaller hydrophobic (Ala > Leu, Ile) or more flexible (Met > Thr) residues are preferred in this position. Furthermore, the α-helical structure is important for the interaction, as a mutation to proline which is expected to disrupt the helix (25) resulted in an inactive T-20 analog.

Circular Dichroism—To clarify the mechanism by which the substitutions at Ser-138 influence the antiviral activity of T-20 derivatives, we examined the binding affinities of these peptides to N-HR using circular dichroism (CD) analysis (Fig. 2). CD spectra reveal the presence of stable α-helical structure of the 6-helix bundle that is a requisite for biological activity and is thought to be mechanistically and thermodynamically correlated with HIV-1 fusion (26). Therefore, CD spectra typically at 222 nm indicate interaction of N-HR (N36) and C-HR (T-20 or C34). Because T-20 does not interact significantly *in vitro* with the N36 peptide, which is derived from amino acids 35–70 of N-HR, we used a derivative of C34, a peptide that overlaps with T-20 and also inhibits HIV fusion by the same mechanism. The C34 derivative contained the analogous T-20 substitutions described above (Fig. 1*B*). Consistent with antiviral activities, a mixture of N36 and $C34_{S138P}$ or $C34_{S138W}$ showed no apparent or reduced α-helicity, respectively. For binding with $N36_{V38A}$

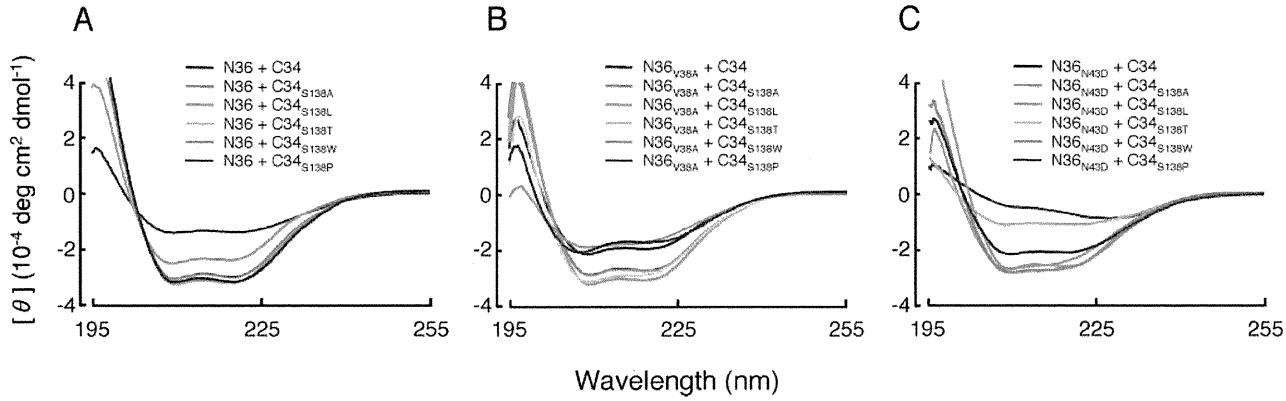

FIGURE 2. **CD spectra of $C34_{S138X}$ complexes with N36 (*A*), $N36_{V38A}$ (*B*), and $N36_{N43D}$ (*C*) are shown.** Equimolar amounts (10 μM) of the N- and C-HR peptides were incubated at 37 °C for 30 min in phosphate-buffered saline. The CD spectra of each mixture were then collected at 25 °C using a Jasco (Model J-710) spectropolarimeter.

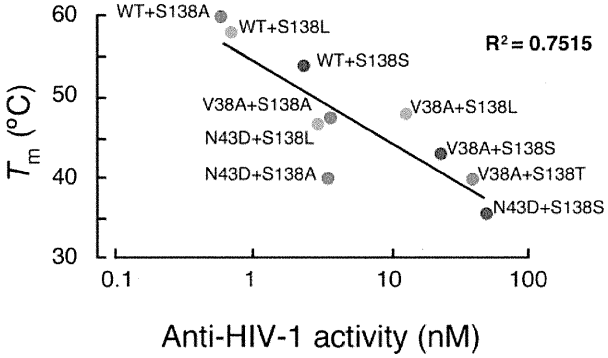

FIGURE 3. **Correlation of T_m values of complexes formed from N36 and C34 peptides (Fig. 2) and anti-HIV-1 activities of $T\text{-}20_{S138X}$ (Table 1).**

or $N36_{N43D}$, sufficient α-helicity at 25 °C was observed only in $C34_{S138A}$, $C34_{S138L}$, and $C34_{S138T}$ or $C34_{S138A}$, $C34_{S138L}$, and $C34_{S138W}$, respectively (Fig. 2, *A–C*).

To determine the thermal stability of the helical complexes formed from the N36 and C34 peptides, we measured the melting temperature (T_m) of each complex (supplemental Table 1). The sigmoidal transition of the CD signal at 222 nm correlates with the thermal stability of the helical complexes formed from the N36 and C34 peptides, which in turn are indicative of the binding affinity of these peptides. The melting temperature (T_m) indicating the 50% disruption of 6-helix bundle was comparatively evaluated. Complexes of N36 and C34 containing the S138A or S138L substitutions ($N36/C34_{S138A}$ or $N36/C34_{S138L}$) showed high thermal stability, comparable with that of the wild-type N36/C34 complex. Similarly, the addition of the S138A or S138L also improved the thermal stability of the $N36_{N43D}$/C34 complex. These results reveal a striking correlation between the thermal stability and the anti-HIV-1 activity of the complexes (R^2 = 0.75, Fig. 3). The low T_m value of the complex formed from $N36_{N43D}$ and C34 suggests that virus containing the N43D mutation shows high resistance to T-20, likely due to less favorable thermodynamics that are expected to drive the formation of the 6-helix bundles containing T-20 inhibitor.

Antiviral Activity of Substituted C34 at Ser-138—To confirm that binding of C34 to N-HR is indeed representative of T-20 binding to N-HR, we examined the anti-HIV-1 activities of

TABLE 2

Antiviral activity of $C34_{N126K}$ peptides against C34-resistant gp41 recombinant viruses

Anti-HIV activity was determined by the MAGI assay. The data shown are the mean values and S.D. that were obtained from the results of at least three independent experiments. Shown in parentheses are the -fold increases in resistance (increase in EC_{50} value) calculated by comparison to a reference virus. The increase of >10-fold is indicated in bold.

	EC_{50}	
	HIV-1_{WT} [a]	HIV-$1_{\Delta V4/I37K/N126K/L204I}$ [b]
	nM	
C34	1.6 ± 0.35	114 ± 29 (71)
$C34_{N126K}$	0.95 ± 0.22 (0.6)	1.1 ± 0.5 (0.7)

[a] To improve the replication kinetics, the D36G mutation, observed in majority of HIV-1 strains, was introduced into the NL4-3 background used in this study (reference virus).

[b] C34-resistant HIV-1 was constructed with the reference virus as described (13). ΔV4 indicates 5 amino acids deletion (FNSTW) in the V4 region of gp120.

C34-derived peptides that have S138A substitutions. The $C34_{S138A}$ and $C34_{S138L}$ peptides showed potent anti-HIV-1 activities, similar to $T\text{-}20_{S138A}$ and $T\text{-}20_{S138L}$ (supplemental Table 2). Based on these findings, we conclude that the stability of complexes comprised of modified C34s and N36s containing T-20 resistance mutations offers a good measure of the binding affinity of $T\text{-}20_{S138X}$ to N-HR.

Antiviral Activity of C34 with N126K—We have recently identified another mutation at the N-HR of gp41 (N126K) during exposure of HIV-1 to C34 *in vitro* (13). The N126K has been occasionally observed after prolonged T-20-containing therapy (10, 15). Here we have confirmed that the $C34_{N126K}$ peptide can also suppress a C34-resistant clone containing several mutations: I37K/N126K/L204I (Table 2). Therefore, peptides designed to have compensatory mutations seem to have potent antiviral activity. However, because residue 126 is located outside the amino acid sequence of T-20 (Fig. 1*B*), we could not examine the effect of N126K substitution on T-20 activity.

Replication Kinetics of Ser-138-substituted HIV-1—To evaluate the effect of Ser-138 substitutions on viral replication, we constructed molecular clones introducing several Ser-138 and determined their replication kinetics by measuring p24 gag antigen production in the culture supernatant. Single nucleotide changes to the TCA codon for Ser-138 may generate 4 amino acid substitutions, Ala, Thr, Leu, Pro, and Trp. As expected, the compensative substitution, S138A, in the T-20

resistance mutation N43D background enhanced replication kinetics of the N43D-containing clone as shown in supplemental Fig. 1. However, in the WT background the S138A appeared to decrease production of p24 as compared with HIV-1_{WT} (Fig. 4). Other substitutions also reduced their replication kinetics. Interestingly, the S138W substitution did not show measurable p24 production. Syncytia induction and single cycle replication kinetics of the Ser-138-substituted HIV-1 were also examined (supplemental Fig. 2). Sizes of syncytia of each virus formed in the MAGI cells (supplemental Fig. 2, *panels A–E*) were associated with p24-normalized single-cycle infectivities (supplemental Fig. 2, *panel F*) and multicycle replication kinetics (Fig. 4). These results suggest that substitutions at Ser-138 are not likely to appear in the absence of T-20 therapy or the emergence of N43D mutation.

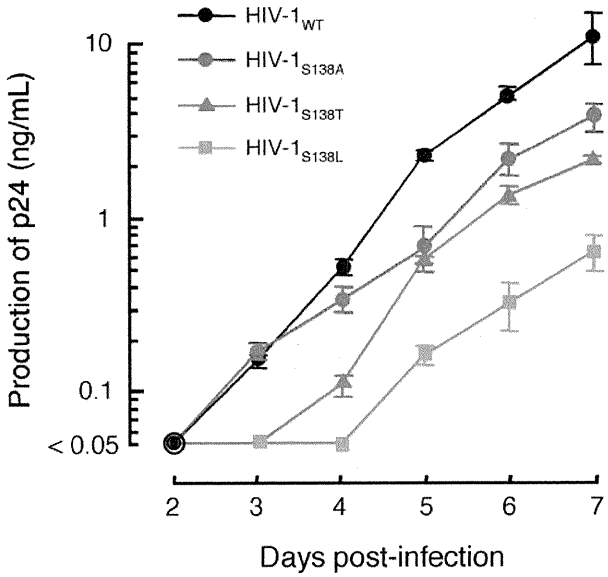

FIGURE 4. **Replication kinetics of HIV-1_{S138X} variants (*X*, any natural amino acid).** HIV-1_{S138A} (*bright red circles*) showed replication kinetics comparable with those seen for HIV-1_{WT} (*blue circles*). Replication of HIV-1_{S138T} (*emerald green triangles*) was reduced, somewhat surprisingly, as both threonine and serine are β-hydroxy amino acids, albeit with different hydrophobicity and torsional flexibility. HIV-1_{S138L} (*orange squares*) also showed reduced replication kinetics. Note that HIV-1_{S138P} and HIV-1_{S138W} failed to replicate (data not shown). Results shown are representative of three independent experiments. An identical order of replication kinetics was observed. Productions of p24 antigen on days 4–7 between HIV-1_{WT} and HIV-1_{S138A} were significant (*t* test, $p < 0.05$).

Structure Modeling—The side chain of amino acid 138 (Ser or Ala) closely contacts with the hydrophobic pocket formed by Leu-44 and Leu-45 in the N-HR. The mutation from Ser to Ala increases hydrophobicity and may help to stabilize the N-HR/C-HR complex related with the potency of the HIV-1 fusion inhibitors (Fig. 5). Larger hydrophobic substitutions such as S138W, S138L, or S138I are likely to sterically interfere with efficient packing of the N-HR and C-HR helices. Similarly, introduction of charged residues at this region of the interface would also disrupt the hydrophobic environment and result in destabilized helix bundles, consistent with the biochemical and virological findings (Figs. 2–4 and Table 1).

Based on crystallographic studies (27, 28), we observe that the T-20 resistance N43D mutation should affect interactions between helices in the 6-helix bundle. Specifically, residue 46 of N-HR is proximal to residue Glu-137 of the C-HR helix of another molecule in the 6-helix bundle. We believe that this increase in proximal negative charges and juxtaposition of Asp-36 next to Glu-137 may destabilize the formation of the 6-helix bundle in a way that results in reduced efficiency of fusion and reduced replication kinetics. Increase of the hydrophobic interactions by introduction of the S138A mutation should help overcome the negative effects of the N43D mutation.

DISCUSSION

In this study we demonstrate that by introducing a secondary resistance mutation into the sequence of peptide-fusion inhibitors such as C34 and T-20, we can suppress efficiently replication of wild-type and of fusion inhibitor-resistant HIV-1. Our circular dichroism analysis revealed that C-HR-based fusion inhibitors that carry secondary resistance mutations can form tight 6-helix bundles with N-HR that contains primary resistance mutations responsible for T-20 resistance. A similar approach has been applied for the development of short hairpin RNA (shRNA) sequences that inhibit HIV-1 replication (29). The synthesized shRNA with mutations that confers resistance to the parental shRNA effectively suppressed replications of shRNA resistant HIV-1 but not wild-type HIV-1. Therefore, it is possible to gain valuable insights from the resistance information and directly apply it to design new peptides or oligonucleotides in the case of shRNA that preempt the viral escape mechanism and suppress resistant variants. Moreover, this strategy should not result in more adverse effect than those that might be obtained during use of the original peptide or oligonucleotide reagents.

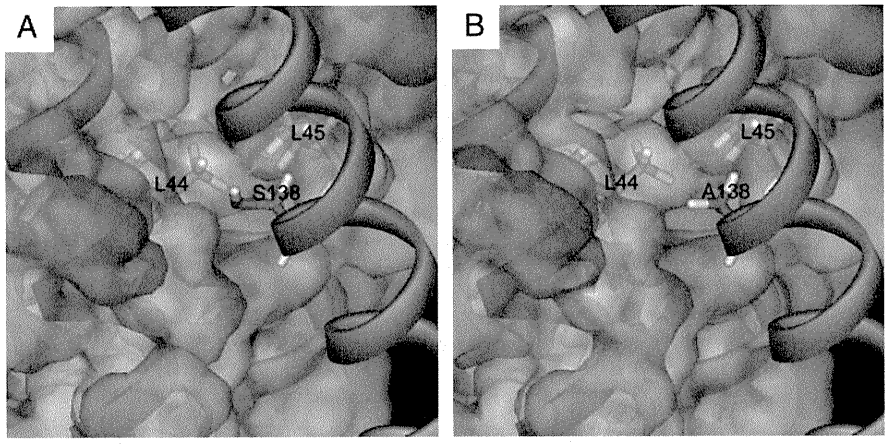

FIGURE 5. **Structure of gp41 at the region near position 138 in the C-HR.** *A*, crystal structure of the N36/C34 complex (PDB code 1AIK). *B*, computational structure modeling of the S138A mutant (N36/$C34_{S138A}$ complex). N-HR and C-HR helices are colored *green* and *orange*, respectively. The van der Waals surface of only N-HR is shown and colored according to the electrostatic potential.

Recently we (6, 30, 31) and others (5) reported that hydrophilic amino

acid substitutions stabilized the α-helix of C-HR peptides and increased their binding affinity to N-HR, thus providing potent anti-HIV activity. This property may be one of the key attributes of the recently developed potent peptide inhibitors, SC34EK (6, 30), T-20EK (31), or T-2429 (5), that have been reported to efficiently inhibit T-20 resistant variants. However, the S138A substitution on T-20 in the present study had little effect on the random coil structure, as judged by CD (data not shown), indicating that $T\text{-}20_{S138A}$ increases its binding affinity not by simply enhancing the α-helicity of this region (5, 6). Our approach of introducing substitutions selected on the basis of the mutation(s) that appears in resistant viruses significantly improved the affinity with N-HR. This approach may complement the effects of enhancing helical stability and may help generate more potent and effective fusion inhibitors for resistant HIV-1 variants.

Other methods have also been employed to improve the potency of HIV fusion inhibitors. For example, T-1249 is a peptide that is based on the T-20 sequence and has improved binding properties (32, 33). It contains 17 changes compared with T-20 (3 additional residues and 14 substitutions to increase the α-helicity/binding affinity according to amino acid sequences of HIV-2 and simian immunodeficiency virus). T-2635 is another efficient peptide fusion inhibitor that was recently developed and is also modified extensively (19 substitutions in 38 amino acids) (5). Also, SC34EK is an electrostatically constrained peptide that also suppresses replication of T-20-resistant variants, and it required 12 substitutions in the original C34 inhibitor (6, 30). Hence, it is possible to improve the potency of existing peptide inhibitors through intense modeling and iterative testing in *in vitro* studies that could lead to the design and synthesis of improved peptide drugs. However, the approach we followed in the design of the $T\text{-}20_{S138A}$ inhibitor is considerably simpler and involves a smaller number of sequence changes (1 residue changed, compared with 19 and 12 in the cases of T-2635 and SC34EK, respectively; see above). It takes advantage of information obtained from the viral evolution under drug pressure and uses the resistance information to design improved inhibitors. In addition, we believe that this approach may be applicable to other targets even when the interactions do not involve helical bundles or detailed information on related systems is not available. Importantly, whenever possible, a combination of the two approaches would likely generate even more effective peptide inhibitors that can suppress replication of resistant variants.

α-Helical structure is a significant factor not only in HIV-1 fusion but also in other examples of protein-protein interactions. Peptide-based drugs have to overcome multiple obstacles, including poor oral bioavailability, less permeability into the target cells, and high cost. Several modifications, such as using arginine-rich peptide tags (34, 35), and chemical treatments (36) have been used to overcome the cell permeability problem. At any rate, peptide-based reagents can be an important tool in the discovery and validation of novel therapeutic targets through *in vitro* experiments. For example, it has been shown that the function of a target protein can be inhibited by designing synthetic peptides that have the amino acid sequence of a domain which is important for the protein function. In such cases the peptides may act as decoys that have antagonistic/agonistic or competitive effects, leading to inhibition of the protein function. Similarly, screening through peptide sequences of proteins may be useful for the identification of functionally important domains that could become future targets for peptide-based or small molecule-based drug development.

In this study we designed peptides tailored to suppress T-20-resistant HIV-1 strains. To our knowledge, this is the first report of direct application of resistance information in drug design and may be applicable to other, unrelated systems. For example, a BH3 domain of the anti-apoptotic protein Bcl-2 has been targeted by an α-helical domain mimic peptide (37, 38). The resulting hydrocarbon-stapled peptide, $SAHB_{A,}$ penetrates into cells via endocytosis pathway and inhibits the function of Bcl-2, inducing apoptosis in transplanted leukemia cells in mice. However, during prolonged therapy with such peptides, leukemic cells could develop resistance to the peptides through substitutions in the Bcl-2 region in the selection process for survival reminiscent of HIV-1. One can envision that our strategy of using mutational resistance information to overcome drug resistance might help in the design of substituted peptides that suppress the resistant variants more efficiently, thus contributing to broader applications of successful peptide-based therapies.

REFERENCES

1. Chan, D. C., and Kim, P. S. (1998) *Cell* **93,** 681–684
2. Weiss, C. D. (2003) *AIDS Rev.* **5,** 214–221
3. Jiang, S., Lin, K., Strick, N., and Neurath, A. R. (1993) *Nature* **365,** 113
4. Chan, D. C., Chutkowski, C. T., and Kim, P. S. (1998) *Proc. Natl. Acad. Sci. U. S. A.* **95,** 15613–15617
5. Dwyer, J. J., Wilson, K. L., Davison, D. K., Freel, S. A., Seedorff, J. E., Wring, S. A., Tvermoes, N. A., Matthews, T. J., Greenberg, M. L., and Delmedico, M. K. (2007) *Proc. Natl. Acad. Sci. U. S. A.* **104,** 12772–12777
6. Otaka, A., Nakamura, M., Nameki, D., Kodama, E., Uchiyama, S., Nakamura, S., Nakano, H., Tamamura, H., Kobayashi, Y., Matsuoka, M., and Fujii, N. (2002) *Angew. Chem. Int. Ed. Engl.* **41,** 2937–2940
7. Lalezari, J. P., Henry, K., O'Hearn, M., Montaner, J. S., Piliero, P. J., Trottier, B., Walmsley, S., Cohen, C., Kuritzkes, D. R., Eron, J. J., Jr., Chung, J., DeMasi, R., Donatacci, L., Drobnes, C., Delehanty, J., and Salgo, M. (2003) *N. Engl. J. Med.* **348,** 2175–2185
8. Lazzarin, A., Clotet, B., Cooper, D., Reynes, J., Arasteh, K., Nelson, M., Katlama, C., Stellbrink, H. J., Delfraissy, J. F., Lange, J., Huson, L., DeMasi, R., Wat, C., Delehanty, J., Drobnes, C., and Salgo, M. (2003) *N. Engl. J. Med.* **348,** 2186–2195
9. Baldwin, C. E., and Berkhout, B. (2006) *Retrovirology* **3,** 84
10. Cabrera, C., Marfil, S., Garcia, E., Martinez-Picado, J., Bonjoch, A., Bofill, M., Moreno, S., Ribera, E., Domingo, P., Clotet, B., and Ruiz, L. (2006) *AIDS* **20,** 2075–2080
11. Labrosse, B., Morand-Joubert, L., Goubard, A., Rochas, S., Labernardiere, J. L., Pacanowski, J., Meynard, J. L., Hance, A. J., Clavel, F., and Mammano, F. (2006) *J. Virol.* **80,** 8807–8819
12. Mink, M., Mosier, S. M., Janumpalli, S., Davison, D., Jin, L., Melby, T., Sista, P., Erickson, J., Lambert, D., Stanfield-Oakley, S. A., Salgo, M., Cammack, N., Matthews, T., and Greenberg, M. L. (2005) *J. Virol.* **79,** 12447–12454
13. Nameki, D., Kodama, E., Ikeuchi, M., Mabuchi, N., Otaka, A., Tamamura, H., Ohno, M., Fujii, N., and Matsuoka, M. (2005) *J. Virol.* **79,** 764–770
14. Perez-Alvarez, L., Carmona, R., Ocampo, A., Asorey, A., Miralles, C., Perez de Castro, S., Pinilla, M., Contreras, G., Taboada, J. A., and Najera, R. (2006) *J. Med. Virol.* **78,** 141–147
15. Xu, L., Pozniak, A., Wildfire, A., Stanfield-Oakley, S. A., Mosier, S. M., Ratcliffe, D., Workman, J., Joall, A., Myers, R., Smit, E., Cane, P. A., Greenberg, M. L., and Pillay, D. (2005) *Antimicrob. Agents Chemother.* **49,**

1113–1119
16. Armand-Ugon, M., Gutierrez, A., Clotet, B., and Este, J. A. (2003) *Antiviral Res.* **59,** 137–142
17. Baldwin, C. E., Sanders, R. W., Deng, Y., Jurriaans, S., Lange, J. M., Lu, M., and Berkhout, B. (2004) *J. Virol.* **78,** 12428–12437
18. Baldwin, C., and Berkhout, B. (2008) *J. Virol.* **82,** 7735–7740
19. Kimpton, J., and Emerman, M. (1992) *J. Virol.* **66,** 2232–2239
20. Maeda, Y., Venzon, D. J., and Mitsuya, H. (1998) *J. Infect. Dis.* **177,** 1207–1213
21. Adachi, A., Gendelman, H. E., Koenig, S., Folks, T., Willey, R., Rabson, A., and Martin, M. A. (1986) *J. Virol.* **59,** 284–291
22. Hachiya, A., Kodama, E. N., Sarafianos, S. G., Schuckmann, M. M., Sakagami, Y., Matsuoka, M., Takiguchi, M., Gatanaga, H., and Oka, S. (2008) *J. Virol.* **82,** 3261–3270
23. Chan, D. C., Fass, D., Berger, J. M., and Kim, P. S. (1997) *Cell* **89,** 263–273
24. Case, D. A., Cheatham, T. E., 3rd, Darden, T., Gohlke, H., Luo, R., Merz, K. M., Jr., Onufriev, A., Simmerling, C., Wang, B., and Woods, R. J. (2005) *J. Comput. Chem.* **26,** 1668–1688
25. Nilsson, I., Saaf, A., Whitley, P., Gafvelin, G., Waller, C., and von Heijne, G. (1998) *J. Mol. Biol.* **284,** 1165–1175
26. Eckert, D. M., and Kim, P. S. (2001) *Annu. Rev. Biochem.* **70,** 777–810
27. Bai, X., Wilson, K. L., Seedorff, J. E., Ahrens, D., Green, J., Davison, D. K., Jin, L., Stanfield-Oakley, S. A., Mosier, S. M., Melby, T. E., Cammack, N., Wang, Z., Greenberg, M. L., and Dwyer, J. J. (2008) *Biochemistry* **47,** 6662–6670
28. Watabe, T., Oishi, S., Watanabe, K., Ohno, H., Nakano, H., Nakatsu, T., Kato, H., Izumi, K., Kodama, E., Matsuoka, M., and Fujii, N. (2009) *Peptide Science*, in press
29. Nishitsuji, H., Kohara, M., Kannagi, M., and Masuda, T. (2006) *J. Virol.* **80,** 7658–7666
30. Nishikawa, H., Nakamura, S., Kodama, E., Ito, S., Kajiwara, K., Izumi, K., Sakagami, Y., Oishi, S., Ohkubo, T., Kobayashi, Y., Otaka, A., Fujii, N., and Matsuoka, M. (September 10, 2008) *Int. J. Biochem. Cell Biol.* 10.1016/j.biocel.2008.08.039
31. Oishi, S., Ito, S., Nishikawa, H., Watanabe, K., Tanaka, M., Ohno, H., Izumi, K., Sakagami, Y., Kodama, E., Matsuoka, M., and Fujii, N. (2008) *J. Med. Chem.* **51,** 388–391
32. Chinnadurai, R., Rajan, D., Munch, J., and Kirchhoff, F. (2007) *J. Virol.* **81,** 6563–6572
33. Eggink, D., Baldwin, C. E., Deng, Y., Langedijk, J. P., Lu, M., Sanders, R. W., and Berkhout, B. (2008) *J. Virol.* **82,** 6678–6688
34. Futaki, S., Suzuki, T., Ohashi, W., Yagami, T., Tanaka, S., Ueda, K., and Sugiura, Y. (2001) *J. Biol. Chem.* **276,** 5836–5840
35. Nagahara, H., Vocero-Akbani, A. M., Snyder, E. L., Ho, A., Latham, D. G., Lissy, N. A., Becker-Hapak, M., Ezhevsky, S. A., and Dowdy, S. F. (1998) *Nat. Med.* **4,** 1449–1452
36. Takeuchi, T., Kosuge, M., Tadokoro, A., Sugiura, Y., Nishi, M., Kawata, M., Sakai, N., Matile, S., and Futaki, S. (2006) *ACS Chem. Biol.* **1,** 299–303
37. Walensky, L. D., Kung, A. L., Escher, I., Malia, T. J., Barbuto, S., Wright, R. D., Wagner, G., Verdine, G. L., and Korsmeyer, S. J. (2004) *Science* **305,** 1466–1470
38. Walensky, L. D., Pitter, K., Morash, J., Oh, K. J., Barbuto, S., Fisher, J., Smith, E., Verdine, G. L., and Korsmeyer, S. J. (2006) *Mol. Cell* **24,** 199–210

THE JOURNAL OF BIOLOGICAL CHEMISTRY VOL. 284, NO. 51, pp. 35681–35691, December 18, 2009
Printed in the U.S.A.

Mechanism of Inhibition of HIV-1 Reverse Transcriptase by 4′-Ethynyl-2-fluoro-2′-deoxyadenosine Triphosphate, a Translocation-defective Reverse Transcriptase Inhibitor*

Received for publication, June 23, 2009, and in revised form, October 14, 2009 Published, JBC Papers in Press, October 16, 2009, DOI 10.1074/jbc.M109.036616

Eleftherios Michailidis[‡], Bruno Marchand[‡1], Eiichi N. Kodama[§2], Kamlendra Singh[‡], Masao Matsuoka[§], Karen A. Kirby[‡], Emily M. Ryan[‡], Ali M. Sawani[‡], Eva Nagy[¶], Noriyuki Ashida[‖], Hiroaki Mitsuya[‡‡], Michael A. Parniak[¶], and Stefan G. Sarafianos[‡3]**

*From the [‡]Christopher Bond Life Sciences Center, Department of Molecular Microbiology and Immunology, University of Missouri, Columbia, Missouri 65211, the [§]Institute for Virus Research, Kyoto University, Kyoto 606-8507, Japan, the [¶]Department of Molecular Genetics and Biochemistry, University of Pittsburgh, Pittsburgh, Pennsylvania 15261, [‖]Yamasa Corporation, Chiba 288-0056, Japan, the **Department of Hematology and Infectious Diseases, Kumamoto University, Kumamoto 860-8556, Japan, and the [‡‡]Experimental Retrovirology Section, HIV/AIDS Malignancy Branch, National Institutes of Health, Bethesda, Maryland 20892*

Nucleoside reverse transcriptase inhibitors (NRTIs) are employed in first line therapies for the treatment of human immunodeficiency virus (HIV) infection. They generally lack a 3′-hydroxyl group, and thus when incorporated into the nascent DNA they prevent further elongation. In this report we show that 4′-ethynyl-2-fluoro-2′-deoxyadenosine (EFdA), a nucleoside analog that retains a 3′-hydroxyl moiety, inhibited HIV-1 replication in activated peripheral blood mononuclear cells with an EC_{50} of 0.05 nM, a potency several orders of magnitude better than any of the current clinically used NRTIs. This exceptional antiviral activity stems in part from a mechanism of action that is different from approved NRTIs. Reverse transcriptase (RT) can use EFdA-5′-triphosphate (EFdA-TP) as a substrate more efficiently than the natural substrate, dATP. Importantly, despite the presence of a 3′-hydroxyl, the incorporated EFdA monophosphate (EFdA-MP) acted mainly as a *de facto* terminator of further RT-catalyzed DNA synthesis because of the difficulty of RT translocation on the nucleic acid primer possessing 3′-terminal EFdA-MP. EFdA-TP is thus a translocation-defective RT inhibitor (TDRTI). This diminished translocation kept the primer 3′-terminal EFdA-MP ideally located to undergo phosphorolytic excision. However, net phosphorolysis was not substantially increased, because of the apparently facile reincorporation of the newly excised EFdA-TP. Our molecular modeling studies suggest that the 4′-ethynyl fits into a hydrophobic pocket defined by RT residues Ala-114, Tyr-115, Phe-160, and Met-184 and the aliphatic chain of Asp-185. These interactions, which contribute to both enhanced RT utilization of EFdA-TP and difficulty in the translocation of 3′-terminal EFdA-MP primers, underlie the mechanism of action of this potent antiviral nucleoside.

Nucleoside reverse transcriptase inhibitors (NRTIs)[4] are central components of first line regimens for treatment of HIV infections (1–6). Currently, there are eight clinically approved NRTIs: AZT, 3TC, FTC, ABC, ddI, ddC, d4T, and the nucleotide tenofovir (TFV; reviewed in Refs. 7 and 8). A structural hallmark of these NRTIs is the lack of a 3′-OH; it has long been considered that the absence of the 3′-OH is essential for antiviral activity. However, the absence of the 3′-OH in NRTIs also imparts detrimental properties to the inhibitor, including reduced affinity for RT compared with the analogous dNTP substrate, as well as reduced intracellular conversion to the active nucleoside triphosphate (9).

Previously we described a series of 4′-substituted NRTIs (10) that retain the 3′-OH group and have excellent antiviral properties and significantly improved selectivity indices (CC_{50}/EC_{50}) compared with the approved NRTIs. Furthermore, these NRTIs efficiently suppress various NRTI-resistant HIV. The most potent of these 4′-substituted NRTIs are the adenosine analogs that have an ethynyl group at the 4′ position of the ribose ring. Despite their high anti-HIV activity, 4′-substituted compounds are susceptible to degradation by adenosine deaminase (11), a property that limits the plasma and intracellular half-life of the drugs. To overcome the adenosine deaminase sensitivity of these 4′-ethynyl NRTIs, we developed a second generation of analogs substituted at the 2-position of the adenine ring (12). We recently reported that the 2-halogenated, 4′-ethynyl compounds have remarkably improved potency and selectivity indices (CC_{50}/EC_{50}) compared with the nonhalogenated analogs and significantly better ones compared with

* This work was supported, in whole or in part, by National Institutes of Health Grants AI076119, AI074389, AI076119-S1, and AI076119-02S1 (to S. G. S.) and AI079801 (to M. A. P.).

[1] Recipient of the amfAR Mathilde Krim Fellowship.
[2] Present address: Div. of Emerging Infectious Diseases, Tohoku University School of Medicine, Sendai 980-8575, Japan.
[3] To whom correspondence should be addressed: 471d Christopher S. Bond Life Sciences Ctr., 1201 Rollins St., Columbia, MO 65211. Tel.: 573-882-4338; E-mail: sarafianoss@missouri.edu.

[4] The abbreviations used are: NRTI, nucleoside reverse transcriptase inhibitor; TDRTI, translocation-defective RT inhibitor; RT, reverse transcriptase; HIV, human immunodeficiency virus; EFdA, 4′-ethynyl-2-fluoro-2′-deoxyadenosine; MP, monophosphate; TP, triphosphate; AZT, azidothymidine; EdA, 4′-ethynyl-2′-deoxyadenosine; EFddA, 4′-ethynyl-2-fluoro-2′,3′-dideoxyadenosine; EFd4A, 4′-ethynyl-2-fluoro-2′,3′-dihydro-2′,3′-dideoxyadenosine; Ed4T, 4′-ethynyl-2′,3′-dihydro-3′-deoxythymidine; TFV, tenofovir; PBMC, peripheral blood mononuclear cell; T/P, template/primer; $T/P_{EFdA\text{-}MP}$ or $T/P_{ddA\text{-}MP}$, template/primer possessing either EFdA-MP or ddAMP at the 3′-primer terminus (or T/P chain terminated by EFdA or ddA); N-site, nucleotide-binding site; P-site, primer site; PDB, Protein Data Bank; d4T, stavudine.

TABLE 1

DNA and RNA sequences used in this study

The primers were fluorescently labeled at the 5′-end except for the footprinting experiments, in which the template was fluorescently labeled at the 5′-end.

Polymerization experiments	
T_{d100}	5′-TAG TGT GTG CCC GTC TGT TGT GTG ACT CTG GTA ACT AGA GAT CCC TCA GAC CCT TTT AGT CAG TGT GGA AAA TCT CTA GCA GTG GCG CCC GAA CAG GGA C
P_{d18}	5′-Cy3 GTC CCT GTT CGG GCG CCA
T_{d31}	5′-CCA TAG CTA GCA TTG GTG CTC GAA CAG TGA C
T_{r31}	5′-CCA UAG CUA GCA UUG GUG CUC GAA CAG UGA C
P_{d18}	5′-Cy3 GTC ACT GTT CGA GCA CCA
Gel shift experiments	
T_{d43}	5′-AAT CAG TGT AGA CAA TCC CTA GCA TTG GTG CTC GAA CAG TGA C
P_{d18}	5′-Cy3 GTC CCT GTT CGG GCG CCA
Footprinting experiments	
P_{d20}	5′-TTG TCA CTG TTC GAG CAC CA
T_{d43}	5′-Cy3 CCA TAG CTA GCA TTG GTG CTC GAA CAG TGA CAA TCA GTG TAGA

other approved NRTIs. These compounds are resistant to degradation by adenosine deamination (13). The most potent of these compounds is EFdA (Fig. 1*A*), which was recently shown not to inhibit human DNA polymerases α and β or mitochondrial DNA polymerase γ (12). Notably, clinically important drug-resistant HIVs (14, 15) are sensitive or hypersensitive to this compound (13).

Despite its remarkable antiviral potency, the molecular mechanism by which EFdA and related compounds inhibit HIV is unknown. To elucidate this mechanism we carried out biochemical experiments that systematically decipher the effect of EFdA on each of the mechanistic steps of DNA synthesis by HIV RT. On the basis of these experiments we propose that EFdA-5′-triphosphate (EFdA-TP) inhibits RT by first being incorporated at the 3′-primer terminus, and after its incorporation it prevents further addition of nucleotides by blocking the translocation of the primer strand on the viral polymerase. We therefore termed EFdA a "translocation-defective reverse transcriptase inhibitor (TDRTI)." By understanding the molecular details of RT inhibition by a highly potent NRTI, we hope to gain insights into the design of even more efficacious inhibitors that may act via same or similar mechanisms.

EXPERIMENTAL PROCEDURES

Enzymes and Nucleic Acids

The RT genes coding for p66 and p51 subunits of BH10 HIV-1 were cloned in the pETDuet-1 vector (Novagen) using restriction sites NcoI and SacI for the p51 subunit and SacII and AvrII for the p66 subunit. The sequences coding for a hexahistidine tag and the 3C protease recognition sequence were added at the N terminus of the p51 subunit. RT was expressed in BL21 (Invitrogen) and purified by nickel affinity chromatography and MonoQ anion exchange chromatography (16). Oligonucleotides used in this study were synthesized chemically and purchased from Integrated DNA Technologies (Coralville, IA). Sequences of the DNA/RNA substrates are shown in Table 1. Deoxynucleotide triphosphates and dideoxynucleotide triphosphates were purchased from Fermentas (Glen Burnie, MD). EFdA was synthesized by Yamasa Corp. (Chiba, Japan) as described previously (12). Using EFdA as the starting material, the triphosphate form, EFdA-TP, was synthesized by TriLink BioTechnologies (San Diego, CA). Concentrations of nucleotides and EFdA-TP were calculated spectrophotometrically on the basis of absorption at 260 nm and their extinction coefficients. All nucleotides were treated with inorganic pyrophosphatase (Roche Diagnostics) as described previously (17) to remove traces of PP_i contamination that might interfere with the rescue assay.

Cell-based HIV-1 Replication Assays

Peripheral blood mononuclear cells (PBMCs) were isolated from healthy donor buffy coats (purchased from the Central Blood Bank, Pittsburgh, PA) using Ficoll-Hypaque (Histopaque, Sigma-Aldrich) gradient centrifugation as described previously (18). PBMCs were stimulated with 5 μg/ml phytohemagglutinin (Sigma) in RPMI 1640 containing 10% fetal bovine serum for 48 h prior to exposure to drug and virus. After washing, the activated cells were resuspended in RPMI 1640/fetal bovine serum containing interleukin-2 (10 units/ml) and varying concentrations of the NRTIs and then were infected with HIV-1_{NL4-3} at a multiplicity of infection of 0.01. HIV-1 infection was assessed by measuring HIV-1 p24 antigen in cell-free culture supernatants obtained 7 days post-infection using an HIV-1 p24 antigen capture assay kit (SAIC, Frederick, MD).

Primer Extension Assays

Characterization of EFdA-TP as a Chain Terminator—DNA or RNA template was annealed to a 5′-Cy3-labeled DNA primer (3:1 molar ratio). To monitor the primer extension, the DNA/DNA or RNA/DNA hybrid (20 nM) was incubated at 37 °C with HIV-1 RT (20 nM) in a buffer containing 50 mM Tris (pH 7.8) and 50 mM NaCl (RT buffer). Subsequently, varying amounts of EFdA-TP or ddATP were added, and the reactions were initiated by the addition of 6 mM $MgCl_2$ to a final volume of 20 μl. All dNTPs were present at a final concentration of 1 μM. The reactions were terminated after 15 min by adding an equal volume of 100% formamide containing traces of bromphenol blue. The products were resolved on a 15% polyacrylamide 7 M urea gel. In this and subsequent assays, the gels were scanned with a phosphorimaging device (FLA 5000, FujiFilm). The bands for fully extended product were quantified using Multi Gauge software (FujiFilm), and the results were plotted as percent full extension using GraphPad Prism 4 to determine the IC_{50} for EFdA-TP and other nucleotide analogs.

Steady State Kinetics—Steady state kinetic parameters, K_m and k_{cat}, for incorporation of EFdA-MP or dAMP were determined using single nucleotide incorporation in gel-based assays under saturating substrate conditions. The reactions were car-

ried out in RT buffer with 6 mM $MgCl_2$, 100 nM T_{d31}/P_{d18} or T_{r31}/P_{d18}, and 2.5 nM RT in a final volume of 20 μl and stopped at the indicated reaction times. The products were resolved and quantified as described above. K_m and k_{cat} were determined graphically using the Michaelis-Menten equation.

Incorporation of dNTP to the Template/Primer (T/P) Possessing Either EFdA-MP (T/$P_{EFdA\text{-}MP}$) or ddAMP (T/P_{ddAMP}) at the 3′-Primer Terminus—$T/P_{EFdA\text{-}MP}$ and T/P_{ddAMP} were prepared by incubating 500 nM T_{d31}/P_{d18} with 1 μM HIV-1 RT in RT buffer and 6 mM $MgCl_2$. EFdA-TP (1 μM) or ddATP (5 μM) was added into the reaction and the mixture was incubated at 37 °C for 1 h. After incorporation of the nucleotide analogs, the T/P_{analog} was purified using the QIAquick nucleotide removal kit (Qiagen, Valencia, CA). Under these conditions, the extension of T/P to $T/P_{EFdA\text{-}MP}$ or T/P_{ddAMP} was complete. Purified $T/P_{EFdA\text{-}MP}$ (5 nM) was incubated with 20 nM HIV-1 RT in RT buffer and 6 mM $MgCl_2$. The first incoming nucleotide was added at different concentrations (0–100 μM) in the presence of the other dNTPs (1 μM). The reactions were incubated at 37 °C for 15 or 60 min.

Gel Mobility Shift Assays

Formation of RT·DNA Binary Complex—$T/P_{EFdA\text{-}MP}$ and T/P_{ddAMP} were prepared using T_{d43}/P_{d18} as described above. Purified $T/P_{EFdA\text{-}MP}$ or T/P_{ddAMP} (20 nM) was incubated at room temperature for 10 min with different concentrations of HIV-1 RT in RT buffer and 6 mM $MgCl_2$. RT was used at different concentrations to obtain RT/DNA ratios that ranged from 0.25 to 7.5. Four μl of 20% sucrose was added to each mixture in a final volume of 20 μl. The complexes were subsequently resolved on a native 6% polyacrylamide Tris borate gel and visualized as described above.

Formation of RT·$DNA_{EFdA\text{-}MP}$·dTTP Ternary Complex—Purified $T/P_{EFdA\text{-}MP}$ or T/P_{ddAMP} (9 nM) was incubated at room temperature for 10 min with 100 nM HIV-1 RT, varying amounts of the next nucleotide (1–5000 μM) in RT buffer, and 6 mM $MgCl_2$. Prior to the addition of sucrose, 150 ng/μl heparin was added, and finally the products were resolved on native 6% polyacrylamide Tris borate gels and visualized as described above.

Site-specific Fe^{2+} Footprinting Assay

Site-specific Fe^{2+} footprints were monitored on 5′-Cy3-labeled DNA templates. T_{d43}/P_{d20} (100 nM) was incubated with HIV-1 RT (600 nM) in a buffer containing 120 mM sodium cacodylate (pH 7), 20 mM NaCl, 6 mM $MgCl_2$, and EFdA-TP (1 μM) to allow quantitative chain termination. Prior to treatment with Fe^{2+}, complexes were preincubated for 7 min with increasing concentrations of the next nucleotide as indicated in Fig. 5*A*. The complexes were treated with ammonium iron sulfate (1 mM) as described previously (19). This reaction relies on autoxidation of Fe^{2+} (20) to create a local concentration of the hydroxyl radical, which cleaves the DNA at the nucleotide closest to the Fe^{2+} specifically bound to the RNase H active site.

PP_i- and ATP-dependent Excision and Rescue of $T/P_{EFdA\text{-}MP}$ and T/P_{ddAMP}

PP_i-dependent Excision of $T/P_{EFdA\text{-}MP}$ and T/P_{ddAMP}—Purified $T/P_{EFdA\text{-}MP}$ and T/P_{ddAMP} (20 nM) were incubated at 37 °C with HIV-1 RT (60 nM) in the presence of 150 μM PP_i in RT buffer and 6 mM $MgCl_2$. Aliquots of the reaction were stopped at different times (0–30 min) and analyzed as described above.

PP_i-dependent Rescue of $T/P_{EFdA\text{-}MP}$ and T/P_{ddAMP}—Purified $T/P_{EFdA\text{-}MP}$ and T/P_{ddAMP} (20 nM) were incubated with HIV-1 RT (60 nM) at various concentrations of PP_i (0–150 μM) in RT buffer and 6 mM $MgCl_2$. The assay was performed in the presence of a large excess of competing dATP (100 μM), which prevented reincorporation of EFdA-MP, 0.5 μM dTTP, and 10 μM ddGTP. After an incubation of 10 min at 37 °C, the reactions were stopped and analyzed as described above.

ATP-dependent Rescue of $T/P_{EFdA\text{-}MP}$ and T/P_{ddAMP}—Purified $T/P_{EFdA\text{-}MP}$ and T/P_{ddAMP} (20 nM) were incubated with HIV-1 RT (60 nM) in the presence of 3.5 mM ATP, 100 μM dATP, 0.5 μM dTTP, and 10 μM ddGTP in RT buffer and 10 mM $MgCl_2$. Aliquots of the reaction were stopped at different time points (0–90 min) and analyzed as described above.

Molecular Modeling

Molecular models of two reaction intermediates that involve EFdA were built as follows. 1) A model of the ternary complex of HIV-1 RT·DNA·EFdA-TP (Fig. 7*A*) was built starting with the coordinates of the crystal structure of the HIV-1 RT·DNA·TFV-DP complex. The triphosphate of EFdA-TP was built using as a guide the corresponding atoms of TFV-DP in structure with PDB code 1T05 and of dTTP in PDB code 1RTD. The coordinates of the 4′-ethynyl sugar ring were from our NMR structure of EFdA[5] showing that EFdA is in a North conformation similar to the sugar puckering observed in the crystal structure of 4′-ethynyl-2′-deoxycytidine (21). The structure of the EFdA-TP was assembled from its components using the sketch module of Sybyl 7.0 (Tripos Associates, St. Louis, MO), and minimized by the semiempirical quantum chemical method PM3 (22). The PM3 charges and the docking module of Sybyl 7.0 were used to dock the EFdA-TP at the RT dNTP-binding site (after removing the TFV-DP from 1T05) to generate the ternary complex HIV-1 RT·T/P·EFdA-TP. The final complex structure was minimized for 100 cycles using the AMBER force field with Coleman united charges on the protein and DNA molecules. 2) The model of the RT·$T/P_{EFdA\text{-}MP}$ binary complex with primer 3′-terminal EFdA-MP at the pre-translocation nucleotide-binding site (N-site) (or dNTP-binding site) (Fig. 7*B*) was built using as a starting model our crystal structure of the pre-translocation complex RT·$T/P_{AZT\text{-}MP}$ (PDB code 1N6Q). The structures of AZTMP and the base-pairing dA were replaced by EFdA-MP (built as in EFdA-TP above) and a dT, respectively, using the sketch module of Sybyl 7.0, and energy-minimized using the AMBER force field with Coleman united charges on the protein and DNA molecules.

[5] K. A. Kirby, K. Singh, E. Michailidis, B. Marchand, E. N. Kodama, E. Nagy, N. Ashida, H. Mitsuya, M. A. Parniak, and S. G. Sarafianos, unpublished data.

RESULTS

EFdA-TP Is a Highly Potent Inhibitor of HIV-1 RT—EFdA inhibits HIV-1 replication in phytohemagglutinin-activated PBMCs with an EC_{50} of 50 pM (Table 2), consistent with previously published data obtained using T-cell lines (12, 13), and data published after completion of this work (23). The antiviral potency of EFdA is at least 4 orders of magnitude greater than the clinically used adenine nucleotide analog tenofovir and over 400-fold greater than that of AZT when assessed under the same conditions (Table 2). EFdA thus appears to be the most potent nucleoside inhibitor described to date of HIV-1 replication in primary cells. It is also interesting to note that EFdA is substantially more potent than analogs lacking a 3′-OH function (EFddA and EFd4A; Table 2). No cytotoxicity was noted at 10 μM EFdA (data not shown), the highest concentration tested, suggesting an *in vitro* selectivity index of over 200,000. To better understand the molecular basis for the exceptional antiviral potency of EFdA, we carried out a series of detailed *in vitro* evaluations of the impact of the active antiviral form of EFdA, namely EFdA-TP, on DNA synthesis catalyzed by purified HIV-1 RT.

TABLE 2
Inhibition of HIV-1 replication in phytohemagglutinin-activated PBMCs by EFdA, EFdA analogs, and other NRTIs

Compound	EC_{50}[a]
	nM
EFdA	0.05 ± 0.02
EdA	11 ± 7
EFddA	570 ± 92
EFd4A	14 ± 11
Zidovudine (or AZT)	22 ± 7
Tenofovir	3300 ± 1240

[a] Values are means ± S.D. of triplicate determinations and were determined by assessment of reduction in HIV-1 p24 antigen production in infected cells as described under "Experimental Procedures."

We first compared the effect of EFdA-TP with other NRTI-TPs (ddATP, TFV-DP, AZTTP, and ddCTP) on RT-catalyzed DNA synthesis in *in vitro* primer extension assays using a nucleic acid T/P comprising a 100-nucleotide DNA template annealed to a Cy3–5′-labeled 18-nucleotide DNA primer (Table 1). As shown in Fig. 1*B*, EFdA-TP suppressed full-length DNA synthesis by RT in a dose-dependent manner. EFdA-TP was between ~1 and 2 orders of magnitude more effective at inhibiting RT-catalyzed DNA synthesis than any of the NRTIs evaluated. The IC_{50} for suppression of full primer extension by EFdA-TP was 14 nM using the longer T_{d100}/P_{d18} (Fig. 1, *C* and *D*). To confirm the high efficiency at which RT uses EFdA, we performed single nucleotide incorporation assays under steady state conditions (using T_{d31}/P_{d18} or T_{r31}/P_{d18} as a T/P, Table 1). Our results show that under these conditions the incorporation efficiency (k_{cat}/K_m) of EFdA-TP by RT is twice that for the natural dATP substrate and four times that for ddATP, primarily because of changes in the K_m of RT to these substrates (Table 3). Moreover, we found that the increase in incorporation efficiency of EFdA-TP could be even higher at different nucleic acid sub-

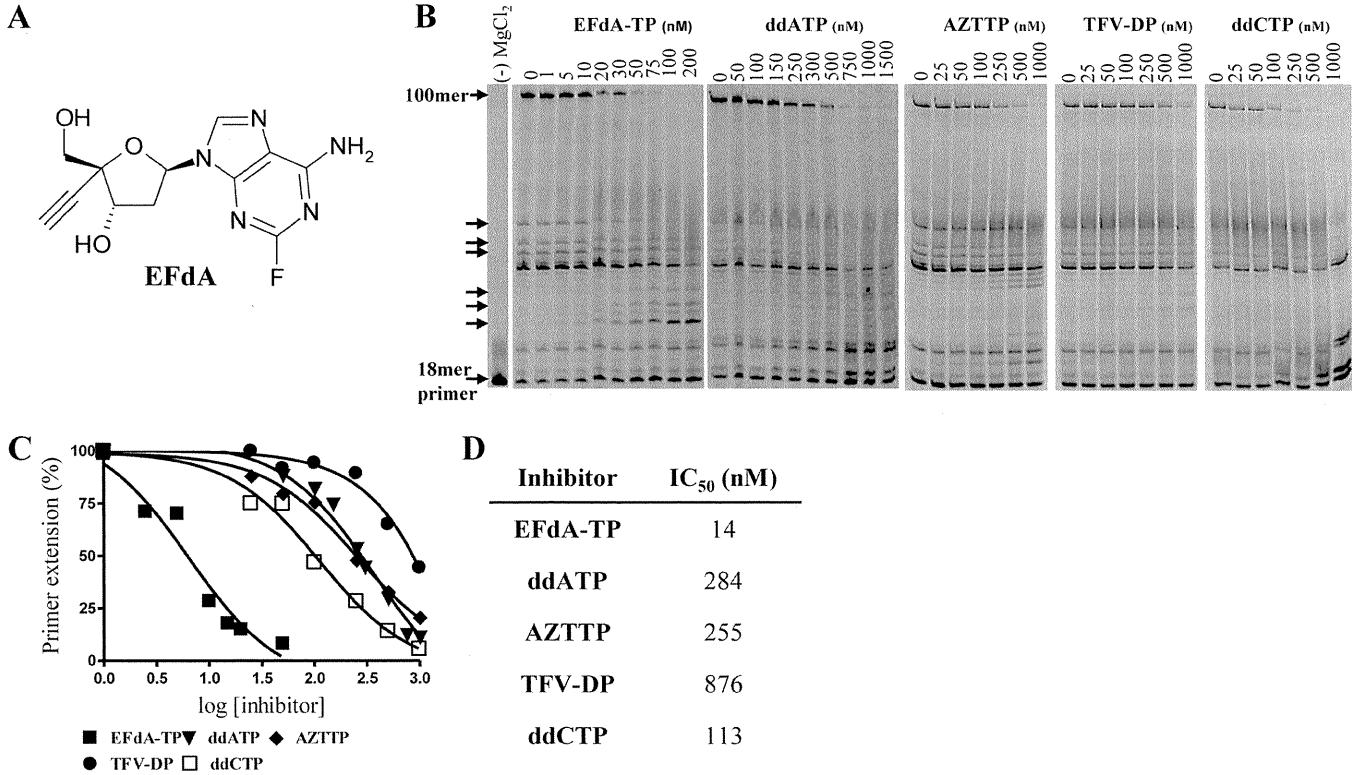

FIGURE 1. **HIV RT inhibition by EFdA-TP and other NRTIs.** *A*, structure of EFdA. *B*, primer extension by HIV-1 RT was observed in the presence of fixed concentrations of 4 dNTPs, T_{d100}/P_{d18}, and $MgCl_2$ and increasing concentrations of EFdA-TP, ddATP, AZTTP, TFV-DP, or ddCTP. The reactions were carried out for 15 min. The *arrows* denote stops of the elongating DNA chain where adenosine analogs (EFdA-TP, ddATP, or TFV-DP) were expected to be incorporated. The *first lane* is a negative control, where no $MgCl_2$ was added; it shows the length of the 18-mer primer. *C*, the 100-mer products synthesized by HIV-1 RT were quantified and plotted against increasing concentrations of various inhibitors. The data points were fitted by GraphPad Prism 4. *D*, IC_{50} values of the nucleotide analogs were determined by quantifying the percent of full extension and fitting the data points to GraphPad Prism 4 using one-site competition nonlinear regression.

TABLE 3

Steady state kinetic parameters (K_m and k_{cat}) for EFdA-MP and dAMP incorporation by HIV-1 RT

Values are means ± S.D. of triplicate determinations and were determined from Michaelis-Menten equation using GraphPad Prism 4. ND, not determined.

dNTP	T/P (DNA/DNA)				T/P (RNA/DNA)			
	K_m	k_{cat}	k_{cat}/K_m	Selectivity[a]	K_m	k_{cat}	k_{cat}/K_m	Selectivity[a]
	nM	min^{-1}	$min^{-1} \cdot nM^{-1}$		*nM*	min^{-1}	$min^{-1} \cdot nM^{-1}$	
dATP	73.11 ± 11	19.9 ± 0.7	0.272	1	21.3 ± 8	3.1 ± 0.2	0.145	1
EFdA-TP	39.2 ± 3	21.1 ± 0.4	0.538	2	24.1 ± 5	2.3 ± 0.1	0.095	0.7
ddATP	97.0 ± 9	15.4 ± 0.3	0.159	0.6	ND	ND	ND	ND

[a] Selectivity is the ratio of the incorporation efficiency (k_{cat}/K_m) of EFdA-MP or ddAMP over that of dAMP ($[k_{cat}/K_m]_{EFdA\text{-}MP}/[k_{cat}/K_m]_{dAMP}$ or $[k_{cat}/K_m]_{ddAMP}/[k_{cat}/K_m]_{dAMP}$).

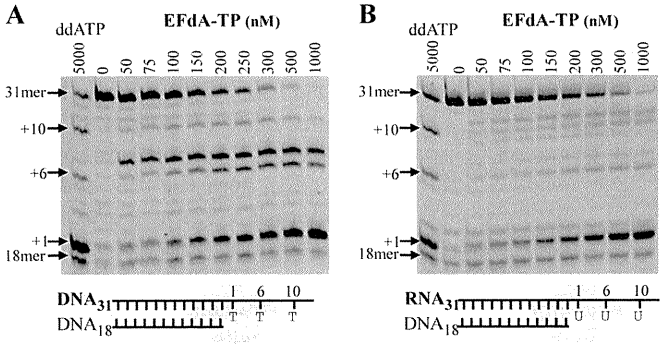

FIGURE 2. **Inhibition of DNA- and RNA-dependent DNA synthesis by EFdA-TP.** *A*, T_{d31}/P_{d18} was incubated with HIV-1 RT for 15 min in the presence of 1 μM dNTPs and $MgCl_2$ and increasing concentrations of EFdA-TP (0–1000 nM). The *first lane* (dd*ATP*) shows the inhibition of primer extension by ddATP to identify points of adenosine analog (ddATP or EFdA-TP) incorporation (*arrows*: +1, +6, and +10). *B*, the primer extension under the same conditions with an RNA/DNA substrate containing an RNA template annealed to a DNA primer (T_{r31}/P_{d18}).

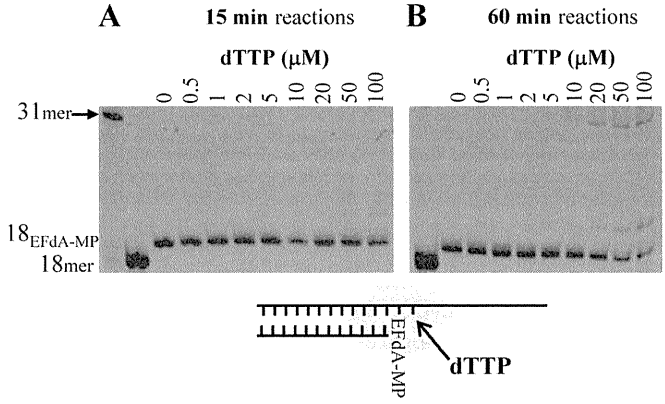

FIGURE 3. **Incorporation of dNTP on EFdA-terminated template/primer ($T/P_{EFdA\text{-}MP}$).** EFdA-TP was first incorporated at T_{d31}/P_{d18} by HIV-1 RT and purified as described under "Experimental Procedures." The incorporation of the next incoming nucleotide on $T/P_{EFdA\text{-}MP}$ was examined in the presence of HIV-1 RT and $MgCl_2$ and increasing concentrations of dTTP. All other dNTPs were at a concentration of 1 μM. The reactions were stopped after 15 min (*A*) and 60 min (*B*).

strate sequences, more than 10 times higher than dATP (data not shown).

The EFdA-TP-mediated reduction in full-length DNA synthesis was accompanied by the concomitant appearance of products corresponding to the primer extension only at the length expected for the incorporation of adenosine nucleotides (indicated by *arrows* in Fig. 1*B*). Neither ddATP nor TFV-DP provided significant accumulation of this small DNA product.

EFdA-TP Inhibits DNA Synthesis Mainly at the Point of Incorporation—The stopping patterns of DNA synthesis were different in the presence of EFdA-TP compared with other dATP analogs such as ddATP and TFV-DP (marked by *arrows* in Fig. 1*B*). Hence, we used a shorter template (T_{d31}/P_{d18} (Table 1)), which allowed unambiguous identification of the stopping sites. As expected, the inhibitory potential of EFdA (and other NRTIs) appears lower in these shorter T/P (IC_{50} for suppression of full primer extension was 104 nM) in which there are fewer opportunities for incorporation (24). This substrate allows incorporation of dA, ddA, or EFdA at positions 1, 6, and 10 (Fig. 2). The results show that EFdA-TP causes major pauses at all possible points of incorporation ((Fig. 2*A*, positions 1, 6, and 10), suggesting that EFdA-TP inhibits RT mainly as an obligate chain terminator. Notably, there was a distinct difference at position +6 of T_{d31}/P_{d18}, where we observed a strong stop not only at the point of incorporation but also at the position following (Fig. 2*A*, positions 6 and 7, respectively). These results suggest that in some cases EFdA-MP may also allow incorporation of an additional nucleotide depending upon the template sequence.

EFdA-TP inhibits both RNA- and DNA-dependent RT-catalyzed full-length DNA polymerization to comparable extents (Fig. 2). The selectivity for incorporation of EFdA-MP over dAMP ($(k_{cat}/K_m)_{EFdA\text{-}TP}/(k_{cat}/K_m)_{dATP}$) was slightly increased when we used DNA/DNA *versus* RNA/DNA template/primers (Table 3, 2 *versus* 0.7). Notably, the overall pausing pattern due to inhibition by EFdA-TP differs depending on whether the template is RNA or DNA. Inhibition differences based on type and sequence of template are currently under investigation.

Extension of EFdA-terminated T/P ($T/P_{EFdA\text{-}MP}$)—The data in Figs. 1 and 2 suggest that EFdA-TP can act as a terminator of RT-catalyzed DNA synthesis in a manner similar to that of other NRTI-TPs. We therefore examined the efficiency of nucleotide additions to primers that were synthesized to already possess a 3′-terminal EFdA-MP. Fig. 3 shows that the primer extension from EFdA-MP is very limited and is evident only at very high and nonphysiological concentrations (>50 μM) of the next nucleotide and with extended reaction times (Fig. 3*B*, 60-min incubation). It therefore appears that EFdA acts as a *de facto* chain terminator, despite the presence of a 3′-OH function.

RT Binds T/P_{ddAMP} and $T/P_{EFdA\text{-}MP}$ at Similar Efficiencies—A possible reason for the inability of RT to efficiently extend the EFdA-MP-terminated primer is that it binds $T/P_{EFdA\text{-}MP}$ with less affinity than it does a T/P lacking a 3′-terminal EFdA-MP nucleotide. We therefore used gel mobility shift assays to compare the stabilities of the binary complexes of RT with T/P possessing either EFdA-MP ($T/P_{EFdA\text{-}MP}$) or ddAMP

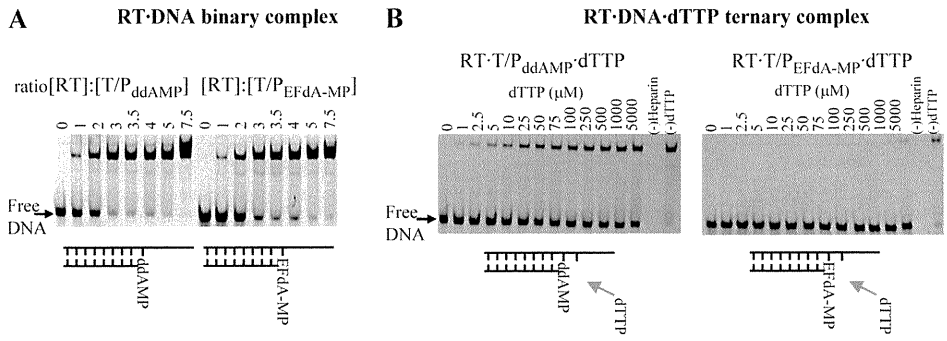

FIGURE 4. **Effect of ddA or EFdA on formation of binary and ternary complexes.** *A*, formation of a binary complex between RT and T/P$_{ddAMP}$ or T/P$_{EFdA-MP}$. Purified T/P$_{ddAMP}$ or T/P$_{EFdA-MP}$ (20 nM) was incubated with HIV-1 RT at the indicated molar ratios and resolved by nondenaturing gel electrophoresis. *B*, formation of a ternary complex between RT and T/P$_{ddAMP}$ or T/P$_{EFdA-MP}$ and incoming dTTP. The stability of the ternary complexes was analyzed by incubating 100 nM RT and 9 nM T/P$_{ddAMP}$ or T/P$_{EFdA-MP}$ in the presence of increasing dTTP concentrations and heparin, which acted as an enzyme trap. In the absence of dTTP, the T/P·RT binary complex is unstable (*lane 0*), as RT dissociates from the T/P and is trapped by heparin.

(T/P$_{ddAMP}$) at the 3′-primer terminus (T/P chain terminated by EFdA-MP or ddAMP). As shown in Fig. 4*A*, RT binds T/P$_{EFdA-MP}$ with an apparent affinity comparable with that of the normal T/P (K_d for RT·T/P$_{EFdA-MP}$ = 51 nM; K_d for RT·T/P$_{ddA-MP}$ = 42 nM). This observation suggests that RT is inhibited at a downstream step in the polymerization reaction.

RT Is Unable to Form a Stable Ternary Complex with T/P$_{EFdA-MP}$ and dNTP—The next step in the DNA polymerization mechanism is the binding of the next complementary dNTP to RT·DNA, thus forming the ternary complex that precedes catalysis. To determine whether EFdA exerts its inhibitory effect by interfering with the formation of a stable ternary complex with the incoming dNTP, we used a gel-based nondenaturing electrophoresis assay (25) that detects the ternary complex formed by RT·T/P and the next complementary dNTP (in this case, dTTP). In this assay, the stability of the ternary complex is assessed by the persistence of the RT·DNA·dNTP complex upon addition of a competing heparin trap (25). As seen in Fig. 4*B* (*left panel*), the ternary complex formed by RT with T/P$_{ddAMP}$ and dTTP is quite stable. In contrast, no significant amount of ternary complex was noted in assays using T/P$_{EFdA-MP}$ even at very high dTTP concentrations (Fig. 4*B*, *right panel*).

Incorporation of EFdA-TP into DNA (T/P$_{EFdA-MP}$) Decreases Translocation of RT—The inability of RT to form a stable ternary complex with T/P$_{EFdA-MP}$ and the next complementary dNTP could arise from several factors including (i) the inability of the 3′-terminal EFdA-MP primer to efficiently translocate from the N-site (which is also the pre-translocation site) to the post-translocation primer site (P-site), thereby preventing the next incoming nucleotide from binding; and (ii) the fact that T/P$_{EFdA-MP}$ *can* translocate, but the presence of unnatural substituents in the primer 3′-terminal EFdA-MP (4′-ethynyl and 2-fluoro) may alter geometric and electronic parameters at the primer end, thus preventing efficient incorporation of the next incoming dNTP such that catalysis cannot occur. These two different possibilities place the nucleic acid at different positions/registers with respect to a site-specific landmark in RT, the metal-binding ribonuclease H (RNase H) active site, as shown in the schematic of Fig. 5*B*. We therefore used a site-specific Fe^{2+} footprinting assay (19) to determine whether the primer 3′-terminal EFdA-MP of the RT·T/P$_{EFdA-MP}$ complex resides primarily in the pre- (N-site) or post-translocation (P-site) state in the absence and the presence of varying levels of the incoming complementary dNTP, which serves to "force" the 3′-primer terminus from the pre-translocation (N-site) to the post-translocation site (P-site). As shown on Fig. 5*A* (*left panel*), in the absence of dTTP (*first lane*), primers with a 3′-terminal ddAMP are located in both the pre- and post-translocation sites in approximately equal amounts, and the addition of the next complementary nucleotide (dTTP) forces the primer 3′-end almost entirely into the post-translocation site. In contrast, in the absence of dTTP, primers with a 3′-terminal EFdA-MP are located exclusively in the pre-translocation site (Fig. 5*A*, *right panel*, *first lane*). The next complementary nucleotide (dTTP) is unable to shift the position of the 3′-EFdA-MP except at very high (nonphysiological) concentrations.

Because it is physically impossible for the incoming dNTP to bind at the N-site (dNTP-binding site) when it is occupied by the 3′-primer terminus of the non-translocated T/P$_{EFdA-MP}$, the present data demonstrate that the apparent termination of RT-catalyzed DNA synthesis upon incorporation of EFdA-MP arises from the inability of the 3′-EFdA-MP-terminated primer/template (T/P$_{EFdA-MP}$) to efficiently translocate to the P-site and allow incorporation of the next dNTP. Moreover, the latter is unable to force translocation of the 3′-EFdA-MP-terminated primer strand. The inability of the 3′-EFdA-MP-terminated primer to translocate to allow binding of the next complementary dNTP effectively prevents continued elongation of the nascent viral DNA, despite the presence of the 3′-OH on EFdA. Therefore, we propose that EFdA acts as a *translocation-defective reverse transcriptase inhibitor.*

Phosphorolytic Excision of EFdA-MP—Two major mechanisms account for HIV resistance to NRTIs (26). One is based on NRTI discrimination, where the mutant RT preferentially incorporates the natural dNTP rather than the NRTI-TP. The other major resistance mechanism involves ATP-mediated phosphorolytic excision of the incorporated chain-terminating NRTI from the 3′-end of the primer (27, 28). We and others have previously shown that for excision to occur, the 3′-end of the primer must be positioned at the pre-translocation or N-site of RT (19, 29, 30). As we have already shown, the 3′-EFdA-MP-terminated primer strand binds predominantly in a pre-translocation mode. This suggests that EFdA-terminated primers might be especially susceptible to RT-catalyzed phosphorolytic removal of the terminating EFdA-MP. To assess this possibility we carried out primer unblocking experiments using nucleic acid substrates having at the 3′-primer terminus either EFdA-MP or ddAMP (T/P$_{EFdA-MP}$ or T/P$_{ddAMP}$, respectively). The quantitation of results in Fig. 6*A*

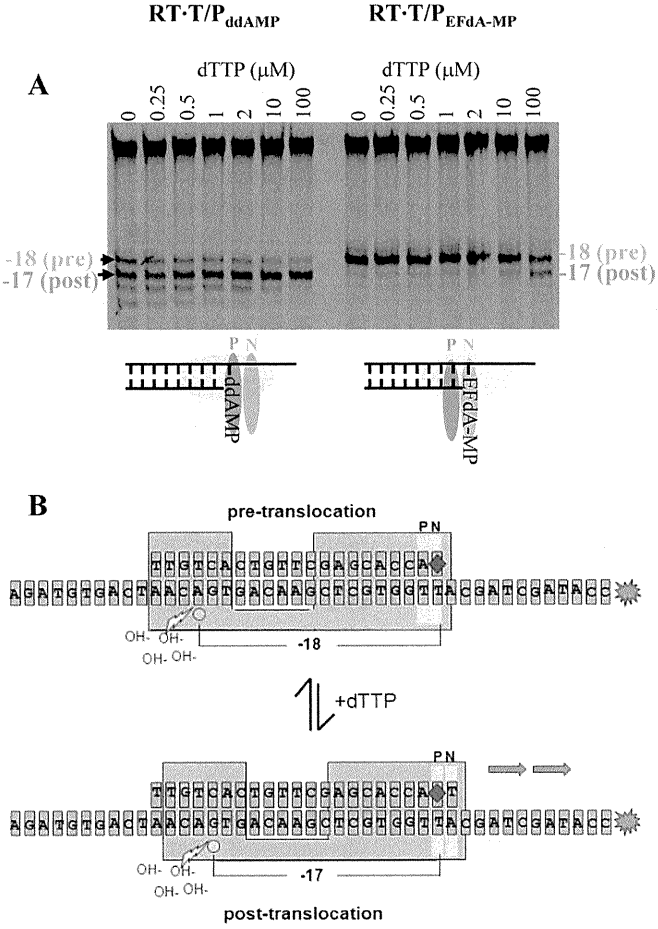

FIGURE 5. **Determination of the translocation state of RT bound to T/P$_{ddAMP}$ and T/P$_{EFdA-MP}$ template/primers.** *A*, the translocation state of RT after EFdA-MP incorporation was determined using site-specific Fe^{2+} footprinting. T/P$_{ddAMP}$ or T/P$_{EFdA-MP}$ (100 nM) with 5′-Cy3 label on the DNA template (see Fig. 5*B*) was incubated with HIV-1 RT (600 nM) and various concentrations of the next incoming nucleotide (dTTP) (as indicated). The complexes were treated for 5 min with ammonium iron sulfate (1 mM) and resolved on a polyacrylamide 7 M urea gel. An excision at position −18 indicates a pre-translocation complex, whereas the excision at position −17 represents a post-translocation complex. The scheme below the gel images indicates that in the absence of incoming dNTP, T/P$_{ddAMP}$ is bound mostly in a post-translocation state, whereas T/P$_{EFdA-MP}$ is bound in a pre-translocation state, with EFdA-MP positioned at the N-site. *B*, schematic of the excision assay. Depending on whether the 3′-primer terminus is positioned at the pre-translocation (N-site) or post-translocation (P-site) site, cleavage is observed on the 5′-labeled template strand at positions −18 or −17, respectively. The addition of varying levels of the incoming complementary dNTP serves to force the 3′-primer terminus from the N-site to the P-site.

shows that the rate of hydrolysis of ddAMP- and EFdA-MP-terminated primers was 0.5 and 1.6 min^{-1}, respectively. We also considered whether the EFdA-TP formed upon pyrophosphorolytic removal of the 3′-terminal EFdA-MP was promptly reincorporated. We tested this possibility using so-called phosphorolysis "rescue" assays, where in addition to the PP_i that would react with the EFdA-MP from the 3′-primer terminus to produce EFdA-TP, we also included a high concentration of dATP that would compete with and prevent reincorporation of EFdA-TP. In the case of high excision activity, we expected to see higher bands corresponding to rescued and extended primers. Indeed, substantially more primer extension was noted in PP_i- or ATP-mediated rescue assays using 3′-terminal EFdA-MP primers (Fig. 6, *C* and *D*, *right panels*) than in assays using primers with 3′-terminal ddAMP (Fig. 6, *C* and *D*, *left panels*). The rate for the ATP-dependent rescue of EFdA-MP-terminated primer was 0.063 min^{-1}. The corresponding rate for the ATP-dependent rescue of the ddAMP-terminated primer could not be calculated because the reaction was very slow. Collectively, these data suggest that 3′-terminal EFdA-MP is phosphorolytically excised more efficiently than ddAMP, consistent with its preferential positioning at the phosphorolysis-susceptible pre-translocation N-site.

Molecular Basis of RT Inhibition by TDRTIs—To understand the molecular basis of RT inhibition by EFdA-TP, we built molecular models of complexes that represent the following intermediates of the DNA polymerization reaction: 1) a pre-catalytic RT·DNA·EFdA-TP ternary complex and 2) a complex that corresponds to the product of EFdA-MP incorporation *prior* to translocation. Previously we had solved crystal structures representing both types of these intermediates for other NRTIs (29, 31), and the model building was guided by the structural characteristics of these complexes. Moreover, we built the EFdA sugar ring in both models in a 3′-endo (North) conformation based on our unpublished NMR experimental data, which clearly show that the equilibrium of the geometries of the EFdA sugar ring overwhelmingly favors the 3′-endo conformation (North). The RT·DNA·EFdA-TP ternary complex model was built using as a starting structure the coordinates of our RT·DNA·TFV-DP crystal structure (PDB code 1T05), not only because it is the highest resolution structure of an RT ternary complex but also because it is the only structure of RT in complex with an analog of deoxyadenosine triphosphate (31). The model of the RT·DNA·EFdA-TP complex represents the step of EFdA-TP binding to the preformed RT·DNA complex (Fig. 7*A*). It had no significant differences from the crystal structures of the ternary complexes of RT with DNA and TFV-DP (PDB code 1T05) or dTTP (PDB code 1RTD). It shows that the 4′-ethynyl of EFdA-TP is favorably positioned in a hydrophobic pocket formed by Ala-114, Tyr-115, Phe-160, and Met-184 and the aliphatic portion of Asp-185. These interactions are similar to those that have been proposed for binding of 4′-Ed4T, a related NRTI thymidine analog that also has a 4′-substitution but no 3′-OH group (32). These interactions are also consistent with the observed high efficiency of EFdA-MP incorporation by RT (Fig. 1*D*). Similar interactions stabilize the RT·DNA$_{EFdA-MP}$ pre-translocation binary complex, which has the primer 3′-terminal EFdA-MP positioned at the N-site (Fig. 7*B*, pre-translocation complex). These favorable interactions are also consistent with the enhanced binding of T/P$_{EFdA-MP}$ in a pre-translocated mode (Fig. 5).

DISCUSSION

The single most distinguishing feature of NRTIs used in HIV therapy is the absence of a 3′-OH. This property results in termination of further viral DNA synthesis upon incorporation of the inhibitor into the nascent viral DNA. We have shown (10, 13) that certain nucleoside analogs that retain the 3′-OH group can exert potent antiviral activity. One of these, EFdA, inhibits HIV-1 replication in PBMCs with a potency that is several orders of magnitude greater than that of any of the current